Doppler Shift Study

of Gamma-rays from the Reaction

^{82}Se (^{7}Li, xnγ)

by

Shewaferaw Solomon

A Thesis

Submitted in Partial Fulfillment for the Requirements

for the Degree of Master of Science in Physics

in the Addis Ababa University

June, 1995

Addis Ababa

ADDIS ABABA UNIVERSITY

SCHOOL OF GRADUATE STUDIES

"DOPPLER SHIFT STUDY OF GAMMA-RAYS FROM THE REACTION ^{82}Se(Li, XNGAMMA)"

By

Shewaferaw Solomon
Department of Physics
Faculty of Science

Approved by the Examining Board

Prof. H.J. Klug, Ext. Examiner

Dr. S. Tesch, Advisor

Dr. Hailezghi T.Mariam, Examiner

ACKNOWLEDGMENT

I am greatly indebted to my advisor Dr. S. Tesch for his help to accomplish this work. I am thankful to Dr. G. Winter from the Rossendorf Spectroscopy group for providing me the data used in this work. I wish to thank Dr. S. Kotelnikov for assistance he rendered in the installation of the software I used for the data analysis and for writing a programme which was necessary to convert the data into a format readable by the software. I am also indebted to Hailu Wolde for giving his time to read this paper and for his valuable suggestions.

I wish also to thank the Ministry of Education of Ethiopia for giving me a sponsorship to pursue my study. My thanks also go to the Graduate School of Addis Ababa University for providing financial support to cover the expenses of the thesis work. I would also like to thank the Physics Department of Addis Ababa University for the cooperation to use the facilities of the department and for many encouragement I was given.

ABSTRACT

If heavy ions react with nuclei, they can be excited to high spin states. This excitation then usually is followed by an emission of a few nucleons and gamma-rays. The gamma-lines from this heavy-ion nuclear reaction undergo Doppler shift because the nuclei produced in the reaction experience a recoil which is capable of incurring a shift on the lines. To study this feature of gamma lines, which is often done in heavy-ion gamma-ray works, especially in lifetime measurements of nuclear excited states, an analysis of gamma-spectra from the reaction ^{82}Se (^{7}Li ,xnγ) measured at 35^0, 37^0, 90^0, 143^0 and 145^0 with respect to the beam direction has been done. The energy of the ^{7}Li ion beam used was 35 MeV. From the analysis energies and intensities of the gamma-transitions are obtained. The 90^0 spectrum which has no Doppler shift to the first order of approximation is used as a reference to find out the shifted lines. Many lines which have a shift in an interval between 1 keV and 4.5 keV are found. A review of literature on related topics such as the application of Doppler shift in lifetime measurement and the description of single particle shell model and collective model to describe nuclear transition probabilities are included.

CONTENTS

I. Introduction

The possibility that the motion of a source of light affects the energy (frequency) of light was pointed out by Doppler in 1842. However, a complete treatment of the effect in electromagnetic radiation was given later at the beginning of the 20th century after the development of the relativistic theory of the Doppler effect – which is based on the Lorentz time transformation. According to this theory, the γ-rays emitted from the nucleus of an atom suffer a change of the frequency when the nucleus is in motion. This is especially significant when the velocity of the nucleus is large enough in comparison with the speed of light. When the recoiling nucleus has a low velocity, the maximum possible Doppler shift will be small but significant otherwise. In many cases of real situations the shift is so small that it is comparable with the instrumental width of the γ-ray peaks. A lineshape analysis of the observed peak is then useless. In this situation one can only measure a shift of the peak centroid. By using heavy-ion induced reactions, however, the velocities of the recoil nuclei are so large that a detailed lineshape analysis can be done. Obviously a complete lineshape analysis leads to more precise conclusions than a simple peak centroid shift.

Nowadays with the development of heavy-ion beams this phenomenon, the Doppler effect, is widely used for nuclear lifetime measurements in the range between 10^{-14} and 10^{-9} s. This time region is experimentally covered by two methods, namely, the Doppler-shift attenuation method (DSAM: 10^{-14} s up to 10^{-11} s) and the recoil distance method (RDM : 10^{-11}s up to 10^{-9} s).

Heavy-ion induced γ-ray spectroscopy has been fruitful in lifetime measurement of the excited states of nuclei because the induced recoil velocities in heavy ion reactions are large enough

to introduce a detectable shift. This is an important reason why heavy-ion beams are widely used in nuclear spectroscopy. With the acceleration of heavy-ion beams beginning from the 60th together with the improvement of γ-ray detection it has become possible to apply the DSAM and RDM for lifetime measurements.

Of course the time range covered by the methods is a small portion of the tremendous range of nuclear lifetimes (10^{-23} s up to 10^{23} s), observed so far. Nevertheless the lifetimes of a large fraction of the bound states happen to have lifetimes within their range of applicability, thus the methods turn out to be very powerful. Heavy-ion γ-ray work, therefore, has been the potential means in lifetime measurements of the excited states of nuclei.

In light of this usefulness in nuclear physics, especially in heavy-ion in-beam γ-ray spectroscopy, it is of great interest to study the phenomenon of Doppler shift of γ-ray lines and their application in lifetime measurements.

In this thesis the Doppler shift of γ-ray lines is investigated from the heavy-ion induced nuclear reaction ^{82}Se (^{7}Li, x$n\gamma$). The spectra investigated were detected at 35^0 , 37^0 , 90^0 , 143^0 and 145^0 with respect to the beam direction. To find the Doppler shifts or broadening of the γ-lines involved comparison between the 90^0 spectrum, which has no Doppler shift in the first order of approximation, with the other ones is made. Under this framework reviews of nuclear γ-ray radiation emission and the principle and application of Doppler effect in lifetime measurement are presented in section II.

The lifetime of a nuclear state which is determined potentially by employing the principle of Doppler shift is inversely proportional to the transition probability that can be calculated by

using different nuclear models. Hence comparison between the theoretical result and the corresponding experimental measurement of lifetime can serve as a good starting point to judge the model used in the theoretical calculation. The results of this thesis are presented in section III.

The spectra are analysed using a programme known as Gamma Activity and Neutron Activation Analysis System (GANAAS), which was prepared by the International Atomic Energy Agency (IAEA). The flow chart of this program is given in appendix A.

II. Literature review

1. Nuclear γ-radiation

Gamma-radiation is the spontaneous emission of γ-quanta by the nucleus. By emitting γ-quanta, the nucleus goes over from an excited state to a state with a lower energy. There are single radiation transitions when the nucleus emits a single quantum and at once goes over to the ground state (see fig.1a), or cascade transitions when the excitation is removed by a successive emission of several γ-quanta (see fig.1b).

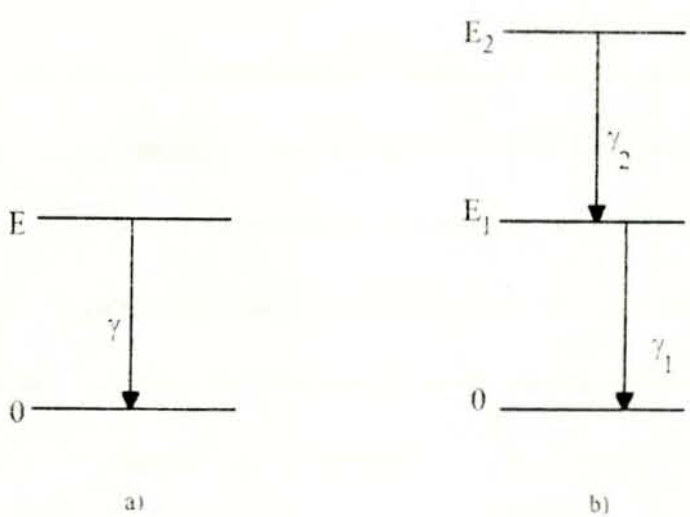

Fig.1 Nuclear γ-transition from one nuclear state to another: a) single radiative transition

b) cascade transition

There are different reasons for which a nucleus may turn out to be in an excited state. For example, the bombardment of a nucleus by ions can leave the formed compound nucleus in an excited state. The nucleus then de-excites by emission of particles accompanied by γ-rays.

The γ-quanta emitted by the nucleus during transition to a lower energy state may carry away different angular momenta l. The radiation carrying angular momenta l=1 is called the dipole radiation, for l=2 it is called the quadrupole radiation, and so on. Each of these radiations is characterized by a definite angular distribution. γ-quanta of different multipolarities are the result of different types of "oscillations" of the nuclear fluid, viz. electric (E1 dipole radiation, E2 quadrupole radiation, and so on) and magnetic (M1 dipole radiation, M2 quadrupole radiation, and so on).

The first type of processes are caused by a redistribution of the electric charges in the nucleus, while the second type of processes are due to a redistribution of the spin and orbital magnetic moments.

A more clear idea about the mechanism of γ-transition can be formed on the basis of specific models of the nucleus. Thus, in the single-particle model, the emission of the γ-multipole is associated with the transition of a nucleon between two single-particle levels differing in their angular momenta by ΔI=l. However, in many cases the single-particle model by itself fails to explain the magnitude of many nuclear electromagnetic transitions. It is very suggestive and plausible that for transitions in which many nucleons contribute in a coherent way (many nucleons "jumping" simultaneously) the transition probability will be different from those transitions where only one nucleon changes its configuration (single-particle transition). In this circumstance the nuclei exhibit collective properties.

1.1 Nuclear models

In general the shell model predicts single-nucleon excitations of the order of 5 to 6 MeV which corresponds to the separation of the main shells. There can occur single particle excitations between subshells which may have lower excitation energy of the order of 1 MeV. But according to the shell model such excitations should occur only for a few neighboring isotopes and isotones. As soon as the subshell is filled up with nucleons, the particles have to be lifted into the next higher subshell which is usually be several MeV away in energy.

There are single-particle transitions (to be described in the shell model) and collective transitions (to be described in the collective model). Low-lying 2^+ states with excitation energies of 0.5 to 1MeV occur very systematically in even nuclei in the neighborhood of closed shells. Furthermore, if more and more protons and neutrons are put into the shell model states, so that both the proton and neutron numbers are far from being magic, these 2^+ states quite systematically appear at energies below 100 keV.

In order to be more specific, let us summarize the experimental observation in the following way. For even-even nuclei two kinds of low-lying positive parity states are observed. One of these is called vibrational, with a typical excitation spectrum as shown in fig.2a, where the 0^+, 2^+, 4^+ triplet has nearly double the excitation energy of the first 2^+ state. This suggests a type of harmonic oscillation where the oscillator quanta each carry an angular momentum of 2h. The observed excited states are just caused by two oscillator quanta coupled to the total spin 0^+, 2^+, or 4^+ [1].

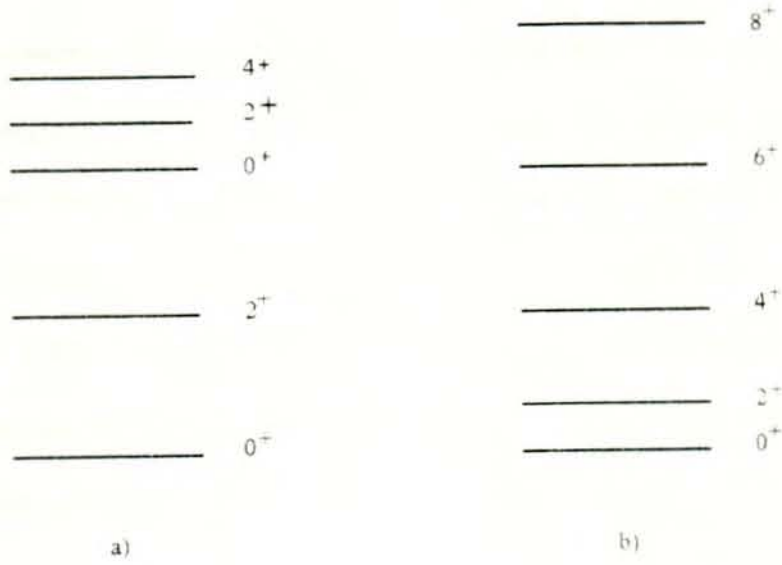

Fig. 2 Typical excitation energy spectrum: a) of a quadrupole surface vibration b) of a rotating nucleus.

The other type of collective states are called rotational. There the various energies of the levels follow roughly an I(I+1) law as shown in fig. 2b. Such a spin dependence in the position of the energy levels suggests immediately the rotational character of the states by analogy to molecular physics. A symmetric rotator will have rotational energy $\varepsilon_I = I(I+1)\hbar^2 / \kappa$ where κ is the moment of inertia.

1.2. γ-ray transition probabilities

In this subsection estimates for the transition probabilities of nuclear levels is presented using a single-particle shell model. The real nucleus, of course, does not follow this simple predictions. However comparing the measured quantities, in particular their relative values, with the corresponding model predictions they can quite often serve as a reasonable starting point for a more refined calculation. Moreover these model predictions are very useful for estimating the size of an effect to be expected in a proposed γ-ray experiment. The γ-transition rate T is given by

$$T = \{ 8\pi (\lambda +1)1 / [h \lambda (2\lambda+1)!!] \} (E_\gamma / hc)^{2\lambda - 1} B (\sigma\lambda) \qquad (1)$$

where B (σλ) is the reduced transition probability. The equation can be derived by using the principles of quantum electrodynamics [1]. The single-particle shell model considers the movement of a single proton or neutron in a spherical potential. The reduce d transition probabilities for electric transitions $B_w(E\lambda)$ and magnetic transitions $B_w(M\lambda)$ according to the Weisskopf estimates are given by the equations

$$B_w (E\lambda) = \{ 9 / [4 \pi (\lambda + 3)^2] \} 1.2^{2\lambda} A^{2\lambda/3} e^2 fm^{2\lambda} \qquad (2)$$

$$B_w (M\lambda) = \{ 90 / [\pi (\lambda + 3)^2] \} 1.2^{(2\lambda - 2)} A^{(2\lambda-2)/3} \mu^2_N fm^{(2\lambda - 2)} \qquad (3)$$

where λ is the order of multipolarity. A is the mass of a nucleus, e is the electron charge, μ_N is nuclear magneton. Using these equations the γ-transition rates T according to Weisskopf estimates can be expressed as indicated in table 1 [2,3].

Table 1 Transition rates in s^{-1} for the lowest electric and magnetic multipoles. $E_{\gamma 0}$ is in MeV.

Eλ	T (Eλ) [s^{-1}]	Mλ	T (Mλ) [s^{-1}]
E1	$1.59 \times 10^{15} E^{3}_{\gamma 0} B_W(E1)$	M1	$1.76 \times 10^{13} E^{3}_{\gamma 0} B_W(M1)$
E2	$1.22 \times 10^{9} E^{5}_{\gamma 0} B_W(E2)$	M2	$1.35 \times 10^{7} E^{5}_{\gamma 0} B_W(M2)$
E3	$5.67 \times 10^{2} E^{7}_{\gamma 0} B_W(E3)$	M3	$6.28 \times 10^{0} E^{7}_{\gamma 0} B_W(M3)$
E4	$1.69 \times 10^{-4} E^{9}_{\gamma 0} B_W(E4)$	M4	$1.87 \times 10^{-6} E^{9}_{\gamma 0} B_W(M4)$

1.3 Gamma transitions and nuclear models for medium and heavy nuclei

A. Electric dipole transitions. A statistical examination of the various transitions is particularly convenient, since it immediately shows the gross properties of electric transitions in nuclei. In fig.3 is plotted the frequency of occurrence of various E1 transition rates, measured in Weisskopf units. From the figure it is seen that the ratio T_{ex} T_W is very small going down to the order of 10^{-9} . This indicates that many of the states have a much more complex structure than what the single-particle model assumes. Besides there also exist states

in nuclei which have very enhanced E1 transition probabilities. These are giant dipole resonances. They are typically of collective nature. The giant dipole resonances form a dipole motion where all protons move in one direction and all neutrons in the opposite direction. This kind of motion produces the largest dipole moments possible in the nucleus and, therefore, very large γ-transition probabilities occur in the decay of the giant resonances.

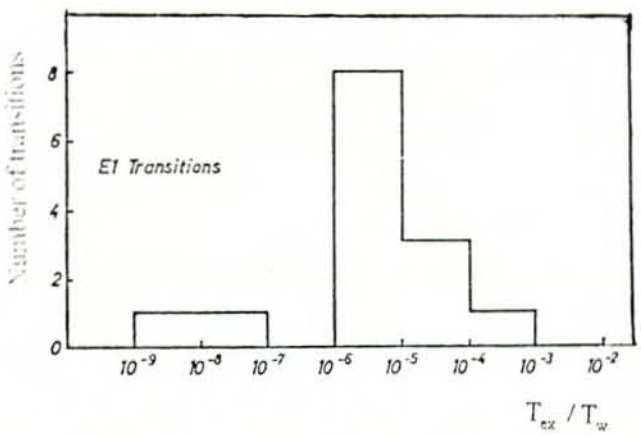

Fig. 3. Frequencies of T_{ex} / T_w, which is the ratio between the experimental to the Weisskopf estimate of lifetime, for E1 transitions in medium and heavy nuclei [3].

B. Electric quadrupole transitions. The statistics for E2 transitions is shown in fig. 4 for medium and heavy nuclei . In contrast to the dipole transitions the E2 transitions are in most cases enhanced by a factor of 10 to 10^3 over the Weisskopf units. This enhancement indicates that there exists a quadrupole-type collective motion because large intrinsic quadrupole moments give rise to nuclear rotations and to strong transition probabilities between the rotational levels.

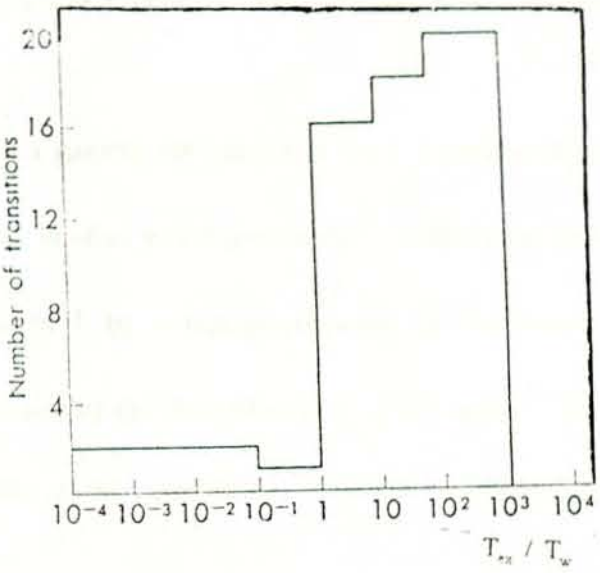

Fig. 4 Frequencies of T_{ex} / T_{w}, which is the ratio between the experimental to the Weisskopf estimate of lifetime, for E2 transitions in medium and heavy nuclei [4].

C. Magnetic Dipole transitions. A statistical examination of M1 transition rates are shown in fig.5. It is seen that the transition rates are smaller than the Weisskopf estimates. This indicates again that the states of the nuclei are not simple independent-particle states but it involve considerable and essential interconfigurational mixing.

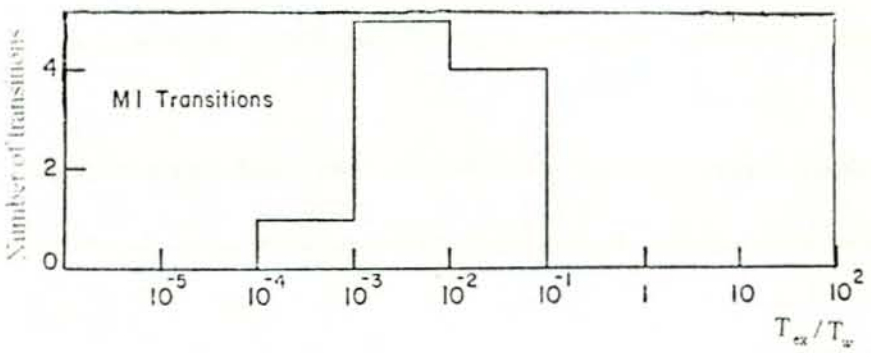

Fig. 5 Frequencies of T_{ex} / T_{w}, which is the ratio between the experimental to the Weisskopf estimate of lifetime, for M1 transitions in medium and heavy nuclei [5].

2. Overview of Techniques for Lifetime Measurements

Consider a gamma ray cascade (Fig.6) passing through an intermediate state having a lifetime τ. In other words emission of γ_2 follows the emission γ_1 after a certain lapse of time governed by τ. In nuclear spectroscopy, the techniques of lifetime measurement allow the determination of the short lifetime τ of the nuclear excited state. By short lifetime we refer to lifetimes in the range of 10^{-14} s - 10^{-6} s, which cannot be determined by direct timing method.

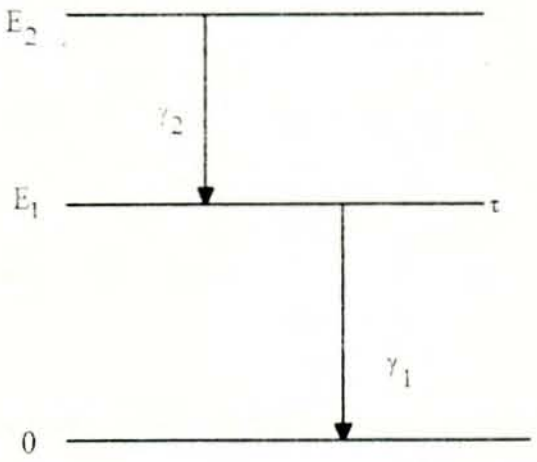

Fig. 6 Gamma-ray cascade passing through an intermediate nuclear level of lifetime τ

There are many methods employed to measure this short nuclear lifetime. The most common ones being electronic methods and recoil methods, as summarised in table 2 [6].

Table 2 Comparison of common life time measurement techniques showing their range of applicability

Method	γ-Energy (MeV)	Nuclear type	Lifetime (sec)
Fast electronics (mainly coincidence)	> 1	All	10^{-6} - 10^{-11}
Nuclear recoil a.. (RDM)	Any	Medium and heavy nuclei	10^{-7} - 10^{-12}
b. (DSAM)	Any	" "	10^{-11} - 10^{-14}

2.1 Electronic Methods

A γ-transition from an excited to a lower nuclear state is always preceded by another nuclear process which produced the excited state. The measurement of the time interval between the two processes determines the lifetime of the nucleus in the radiating state. We can distinguish two different conditions under which such measurements can be made. In the first, which we call "coincidence" method, the succession of transitions is occurring at a steady rate (determined for example by the radioactive decay) and the time of occurrence of the first (as well as the second) process is subject to the usual statistical fluctuations. In the second case which we call the "pulse" method, the excitation occurs at regular, determined time intervals, for example, in a nuclear reaction produced by a succession of short pulses from an

acceleratior so that the instant at which the excited state is produced, within limits, is known exactly. These two types of measurements have much in common as far as technique is concerned. In both cases the γ-radiation from the state being examined is detected, normally by Ge-detectors, and the process registered as a measurable electrical signal before the timing measurement is made. In the coincidence technique the instant at which the radiating state is produced is subject to random fluctuation, and it is determined by detecting the preceding nuclear radiation in a manner which is essentially the same as the detection of the radiation from the state being examined.

Numerous electronic methods have been developed for measuring the time interval between two successive electrical pulses. If the pulses are ideally sharp then time intervals as short as 10^{-11} sec can be measured with fair precision. With a succession of such pair of pulses the average time interval, whether this is constant or subject to some distribution law, can be measured with much higher accuracy of course, since with many measurements there will be a reduction of the random errors associated with a single measurement. In the measurement of the time interval between two nuclear events (or in the case of pulse methods, between the pulse signal and one nuclear event), the nuclear radiation is converted into a measurable pulse only after a succession of processes which introduce time delays and associated uncertainties, and it is these time delays which govern the limits and precision of the measurement.

The electronic timing methods discussed above suffer from the limitation that the events are timed only after the whole complicated processes of detection. The importance of these methods lies in their very general applicability for times greater than about 10^{-11} s. Even

modest improvements in time resolution for such techniques is therefore of a great value. It seems very unlikely that the limits can be extended by much more than an order of magnitude or so. For timing of faster transitions we turn to methods in which the timing is done essentially before the complicated processes in the detector starts, and is not, therefore directly limited by the latter. Together, however, they offer the possibility for measuring γ-transitions over a fairly wide range.

2.2 Recoil Methods (Time of Flight)

There are two recoil methods, namely the Doppler shift attenuation method (DSAM) and the recoil distance method (RDM), as indicated in table 2. Both DSAM and RDM (or with other name plunger technique) are based on the Doppler effect. A detailed description of these two methods is presented in section 3.

2.3 Other Methods

Several other methods have been suggested as possible means of measuring very short nuclear lifetimes. For example if we have γ-radiation following K capture (or a previous γ-transition with a high internal conversion coefficient), then the state of the atomic electrons and in particular the K-shell electrons, at the time of emission of the (second) γ-radiation may be quite different from the normal state. That is, a K-electron level may be unfilled. Measurement of the internal conversion coefficient of this latter γ-ray may then reveal the

abnormal situation in the electronic state. The effect depends on the relative times required for γ-emission by the nucleus and for the electronic transition from the outer shells of the atom to the vacancy in the K-shell. These latter times are in the range 10^{-16} s- 10^{-17} s and can be deduced from line widths in X-ray spectra. This method is applicable only for heavy elements (where large internal conversion is most likely).

3. Description of the Recoil Methods

1. The Recoil Distance Method

The important components of the apparatus used in RDM measurements is the stopper which is usually positioned perpendicular to the beam direction and is separated from the target by a distance d (see fig. 7). The target has to be thin enough for nuclei produced in the target to recoil into the vacuum. For the simplified situation depicted in fig. 7 the number of recoiling nuclei that emit γ-rays before reaching the stopper is measured by the intensity I_F of the γ-rays with Doppler-shifted energy

$$E_\gamma = E_{\gamma 0} [1 + (V / C) \cos \Theta_\Gamma] \qquad (4)$$

The number of nuclei that are stopped before having emitted a γ-ray on their flight paths are identified by the γ-rays having energy $E_{\gamma 0}$ and Intensity I_S. For a pure radioactive decay with lifetime τ, the intensities I_F and I_S are related to the path length d by

$$I_F (d) = I_0 [1 - \exp (- d / v\tau)] \qquad (5)$$

and $$I_S (d) = I_0 \exp(-d / v\tau) \qquad (6)$$

where $I_0 = I_S + I_F$ is the total number of γ-rays.

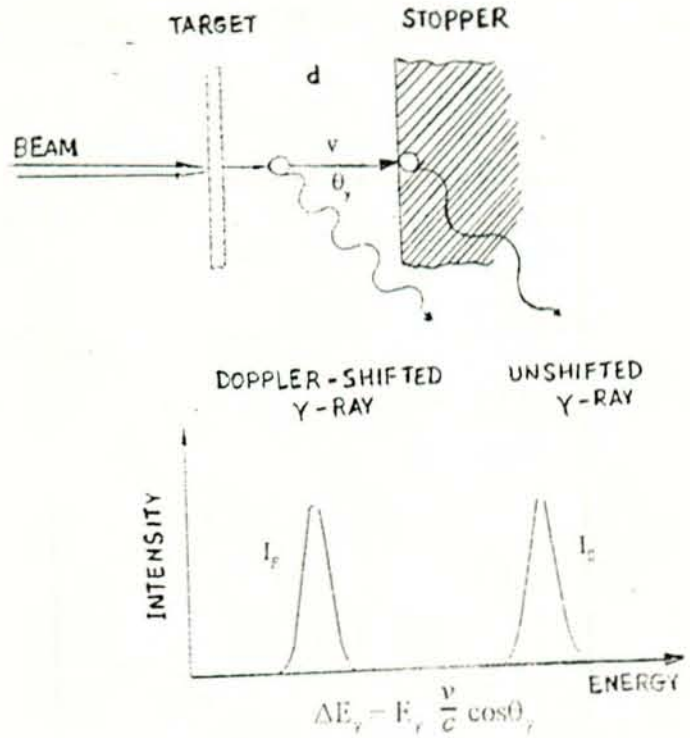

Fig. 7 Principle of measuring lifetimes by the recoil distance method

The ratio R between the stopped intensity I_S and the total intensity $I_S + I_F$ is

$$R(d) = I_S(d) / [I_S(d) + I_F(d)] = \exp[-(d / v\tau)] \qquad (7)$$

or

$$R(d) = \exp[-t_f / \tau] \qquad (8)$$

where $t_f = d / v$ is the flight time. Thus the measurement of $I_S / (I_S + I_F)$ as a function of d (see fig. 8) allows τ to be determined if τ is of the order of t_f. If we assume, for example, τ

is greater or equal to 1ps and v = 0.05 c, half the nuclei have emitted a γ-ray after a path length of greater than or equal to 10 μm, values which can be realised in modern setups.

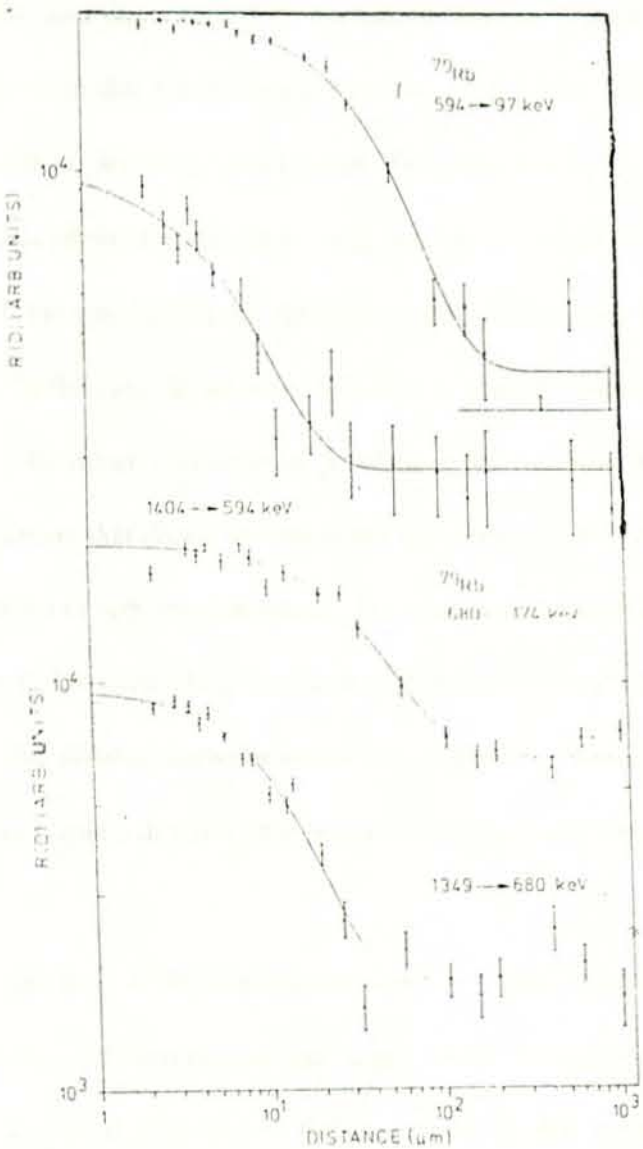

Fig. 8 Recoil distance decay function of some transitions in ^{79}Rb [7]

Note however that a lifetime of τ approximately 1ps is in the order of the slowing-down time in the stopper. Thus the γ-peak will be Doppler broadened. In extreme situations the stopped peak might be so broadened that it cannot be reliably separated from the background. In this case the intensity I_F should be normalised against the total intensity of another γ-ray line in the spectrum that is not Doppler broadened but which originates from the reaction. As these requirements are often hard to meet, the alternative way is to use a thin foil as stopper. The thickness of this foil should be such that the energy of γ-rays emitted after the nuclei have passed through the foil are sufficiently different to allow for a clean separation of the two peaks. In this case the intensity I_S in eq.6 is given by the intensity of the less Doppler-shifted peak. The major experimental problem in RDM measurements is the construction of an arrengement that allows the target and the stopper to be moved in a defined and controllable way down to very small distances. The basic requirements are that the target and the stopper are parallel to each other over an area of at least 0.5 cm^2 , that the parallelity is not destroyed when the distance between target and stopper is changed, and that they can be brought together within a distance of approximately 1μm without them touching each other.

The calibration of the distance between target and stopper is determined by measuring the capacitance between stopper and target. Since the magnitude of a parallel-plate capacitance varies as (1 / d), the plot of the micrometer reading versus the inverse capacitance should give a straight line. This procedure is more accurate than measuring the distance between stopper and foil directly.

The pitfall of RDM measurement lies in its failure to be used in the determination of life time shorter than 10^{-10} s. The slowing down of the recoiling nuclei in the stopper does not occur suddenly but during a time period of 5×10^{-12} s to 5×10^{-13} s. In this period the recoil velocity gradually decreases. This causes a broadening of the stopped component. This phenomenon by itself can be used to determine lifetimes of the order of 10^{-11} s to 10^{-11} s and form another method for lifetime measurement known as DSAM, which is discussed in more detail in the next subsection. In RDM measurements the Doppler broadening of the stopped peak forms a source of systematic errors, and corrections have to be applied in precision measurements where the effective lifetime of the level to be studied is smaller than 10^{-11} s. The calculation of the correction requires either a line-shape analyses of the stopped peak that is shifted or at least a computation of the shifted intensity of the stopped component.

3.2 The Doppler-shift attenuation method

Nuclear lifetimes of the order of 10^{-14} s up to 10^{-11} s can be determined by means of the Doppler-shift attenuation method (DSAM). The method basically consists of comparing the nuclear lifetime with the time in which a nucleus is stopped in solid material (see fig. 9) or gaseous material. The γ-rays that are emitted during the slowing-down process, i.e. at times smaller than the stopping time (t_s) are shifted in their energy according to eq. 4 (considering only first order terms in v/c). On the other hand all nuclei decaying at time t greater or equal to t_s will contribute to the unshifted lines at $E_\gamma = E_{\gamma 0}$.

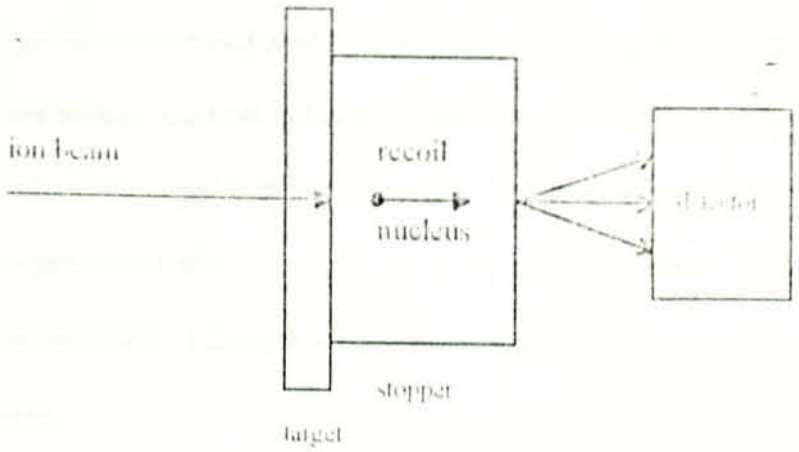

Fig. 9 Schematic representation of Doppler-shift attenuation measurement.

In the DSAM the lifetime of the level is compared with the slowing down time of the recoil nucleus. Usually the centroid energy E_γ of the shifted peak of γ-ray lines is measured as a function of $\cos\Theta_\gamma$. Then the ratio of v to v_0 at which the γ-emission occurs is determined. The Doppler-shift attenuation factor $F = v / v_0$ can be calculated using the stopping theory (v_0 is the initial recoil velocity) [8,9]. Comparing the experimental and theoretical $F(\tau)$ values the lifetime of the decaying state can be determined (see fig. 10).

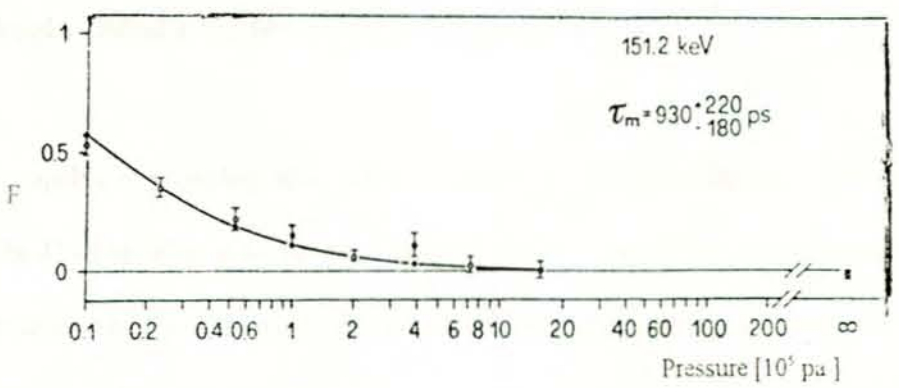

Fig. 10 Experimental attenuation factor F for transition energy of 151.2 keV in ^{71}Rb. The solid curve represents the theoretical F values [7]

The calculation of F (τ) requires knowledge of the slowing-down process at small velocities which is not too well known and hard to treat correctly. It is one of the main advantages of using heavy-ion induced reactions in DSAM experiments that they lead to large initial recoil velocity v_0 where the Doppler shifts are large and easy to measure; and this means the slowing-down process is rather well known. Thus the extracted lifetimes from the analysis of the total γ-ray line-shape obtained from heavy-ion induced reactions are less subjected to systematic errors.

These two methods make use of the Doppler effect phenomenon. One of the main differences between the RDM and the DSAM is in the time scale to which the nuclear lifetimes are compared. The other is that in the RDM the time scale is established by means of the time the excited nuclei with speed v need to travel over a certain distance (where they are stopped in times short compared to the flight time). In the DSAM the nuclear lifetime is compared to the time in which the excited nucleus with speed v is slowed down in solid material. In both techniques the events of γ-emission that occur while the nucleus is still in flight are separated from those that occur after stopping by means of their γ-ray energies which are Doppler-shifted in the first case according to eq. 4.

The RDM is capable of providing more information on the time dependence of the nuclear decay than the DSAM. This is so because the time scale of the RDM can be changed by increasing or decreasing the distance d (distance between target and stopper) whereas in the DSAM the change of the time scale is only possible if the slowing-down material is changed.

The slowing down could also be achieved in a gaseous medium. In this case a change of the gas pressure corresponds to a change of the time scale. However the technique of using

gases as a slowing down medium is not frequently used. Gases cause experimental problems because the slowing-down function of ions in gases is not very well known. One reason for this uncertainty might be, for example, local pressure variations due to local heating of the gas by the beam. To avoid this problem the practical slowing down materials are solids.

The analysis of RDM and DSAM measurements is easiest and the results are most reliable if the excited nucleus has an initial recoil velocity v which is large and well defined in magnitude and direction. It is one of the outstanding features of the heavy-ion induced fusion reactions that the reaction kinematics itself leads to well defined initial recoil velocities of the nuclear residues.

In case v is not uniquely defined, if the differential cross section can be reliably calculated for the reaction, then one can calculate the distribution of recoil velocities and perform the analysis of RDM and DSAM measurements although this analysis is more complicated than in the case where v is uniquely defined.

3.3 Identification of Doppler shifted lines

The identification of Doppler broadened lines has been done by visual inspection of the γ-ray spectrum in conjunction with a careful observation of the form and width of the observed structure compatible with the expected γ-ray lineshape [10,11]. Fig. 11 shows how visual inspection of the lineshape is used to identify the Doppler broadened spectra. The portion of the lines at 45° indicate a broadening when compared to the 90° spectra signifying a Doppler shift.

The γ-lines emitted at 90^0 exhibit no Doppler shift to the first order approximation; and this is a reasonable assumption in in-beam γ-ray spectroscopy studies. Therefore the spectra from the 90^0 measurement is used as a reference to investigate the Doppler shifts obtained from other angles. In the identification of Doppler-shift only those lines with a significant change of lineshape and centroid shift with a clear visual evidence are considered.

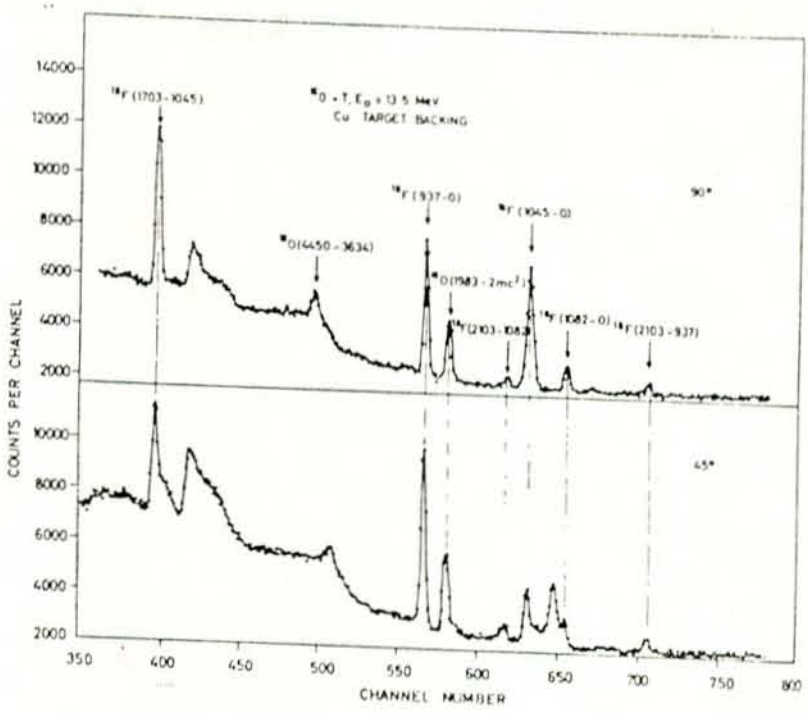

Fig. 11 γ-ray spectra from ^{18}F and ^{18}O measured at 45° and 90°. The target was a layer of TiT on a copper backing. The nuclei ^{18}F and ^{18}O were created in the nuclear reaction $^{16}O + T$ at 13.5MeV with the exit channel $^{18}F + n$ and $^{18}O + p$, respectively. Note particularly the difference of the shapes of the 658-keV line transition from the 1703-keV to the 1045-keV level of ^{18}F [11].

Experimentally it is found that E_γ is directly proportional to $\cos\theta$ [8]. An example is shown in fig. 12. Hence $E_\gamma \sim F\beta\cos\theta$, where $\beta = v_0 / c$.

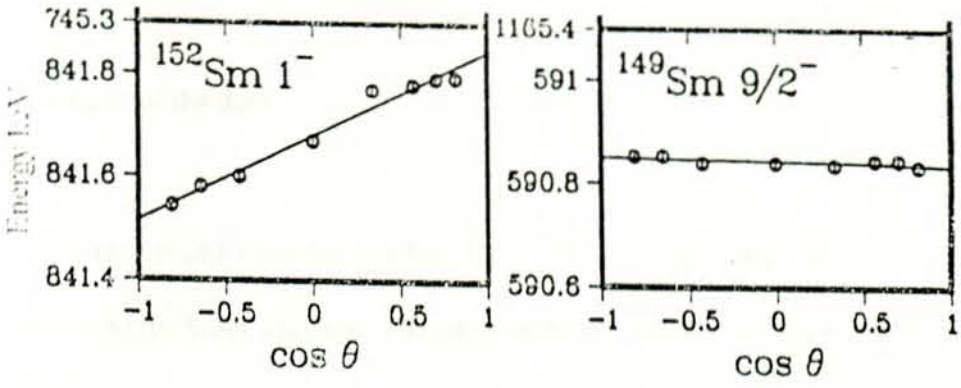

Fig. 12 γ-ray energy versus cos(θ) for selected transitions in Sm isotopes [8]

III. Data Analysis and Results

1. Origin of the data

The γ-ray spectra from the reaction ^{7}Li + ^{82}Se were measured at different detector angles relative to the beam direction. The target material, enriched in ^{82}Se to 92 %, was bombarded by ^{7}Li ions from the Rossendorf Cyclotron (see Fig.13). The measurements were made by means of an intrinsic Ge detector of 10 per cent relative efficiency. The external cyclotron beam of 35 MeV was focussed by a slit or a system of slits and bombarded the target material. The positioned Ge detector at the prescribed angles is then used to detect the radiation.

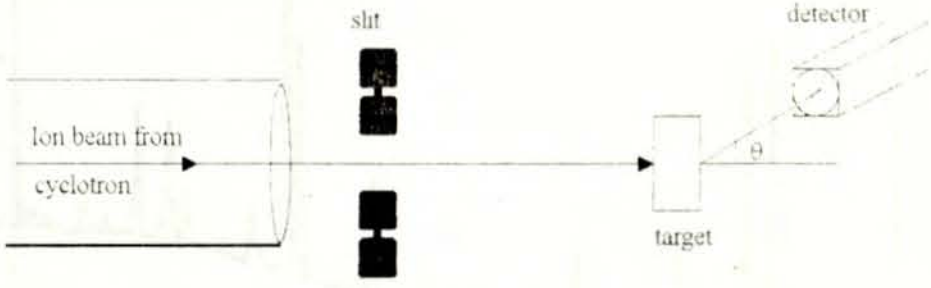

Fig. 13 Schematic diagram of the experimental set-up used in the data taking.

The data in this work , spectra from the reactions ^{82}Se (^{7}Li, xn) at 35^{0} , 37^{0} , 90^{0} , 143^{0} and 145^{0} have been obtained from an experiment conducted recently in the Rossendorf Research Center. Since the spectra received are not manageable by the software available here, a

Pascal program, given in appendix A, was written to transform the data into a form appropriate for the analysis. Examples of the spectra are shown in fig. 14.

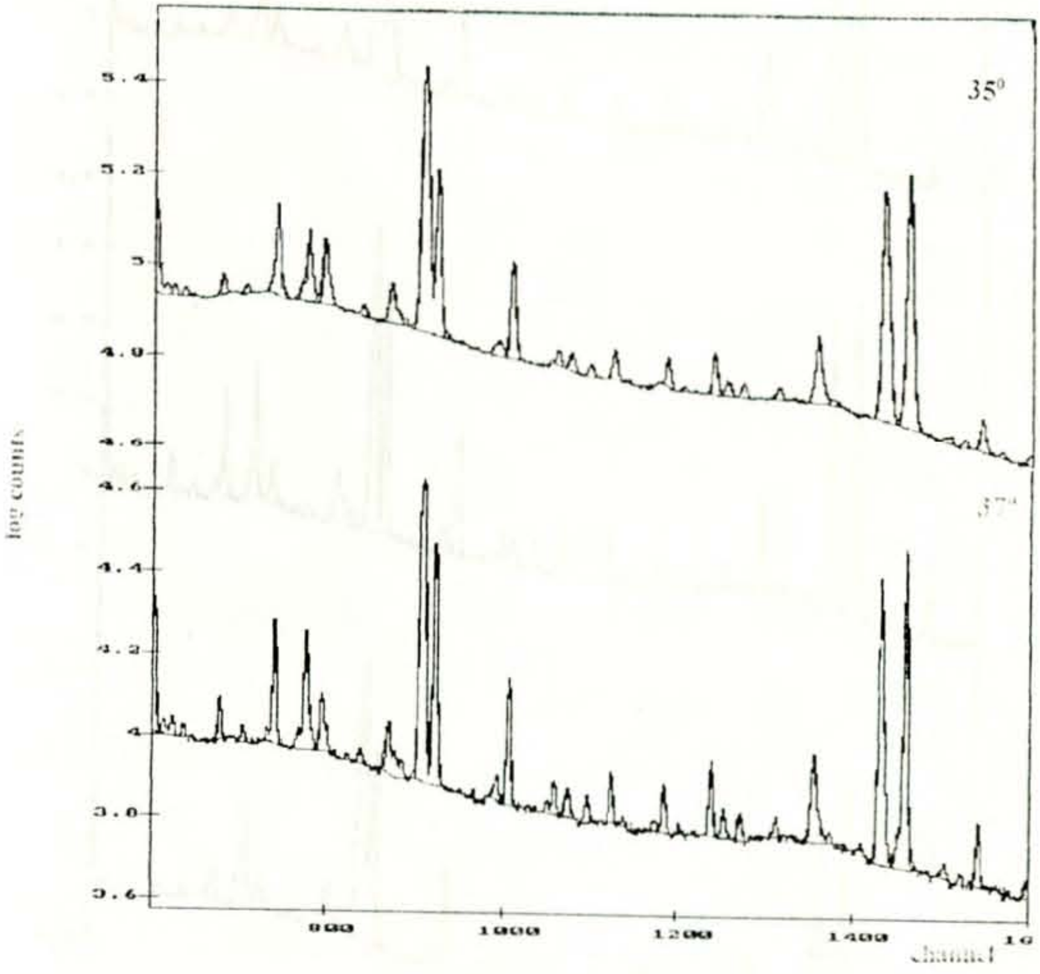

Fig. 14a Portion of γ-ray singles spectra of the reaction [illegible] at angles of 35 [illegible]. The fittings for the full-energy peak and background of the spectra [illegible]

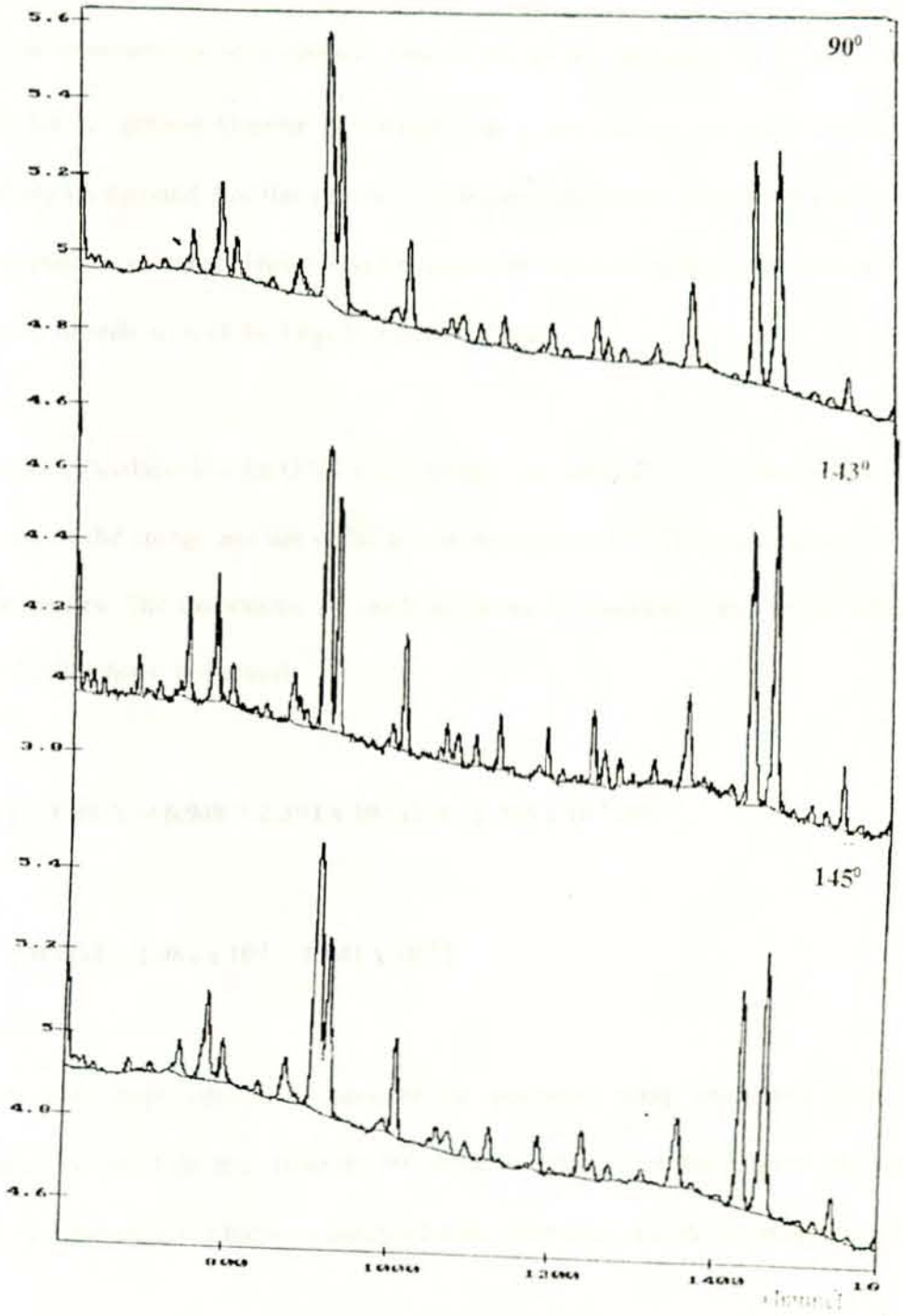
90°
143°
145°
log counts
channel

2. Description of the analysing techniques

The techniques for analysing Doppler broadened γ-ray spectra are not as well developed as those for unbroadened γ-ray spectra. This is due to the difficulties in defining universal criteria for recognizing Doppler broadened γ-ray peaks and for the determination of the underlying background. For this reason an active interplay between personal judgement and the computer is essential. This demand is especially reflected in the calibration procedures and in the identification of the Doppler broadened lines.

In analysis procedures like the GANAAS package (see appendix A) the first step taken is to make use of the energy and full width at half maximum (FWHM) calibrations for setting the parameters. The calibrations are made according to equation 9 and 10 for energy and FWHM calibrations, respectively.

$$\text{ENERGY} = 6.948 + 2.394 \times 10^{-1}\ \text{ch \#} - 1.906 \times 10^{-8}\ \text{ch\#}^2 \qquad (9)$$

$$\text{FWHM} = 2.984 \times 10^{-1} + 1.841 \times 10^{-3}\ E_\gamma \qquad (10)$$

Thirteen lines were selected to perform the parameter setup procedure from energy calibration. Some of the lines from the 90^0 spectrum selected for this purpose are shown in Fig.15. A complete list of the lines selected for the other spectra is shown in appendix B.

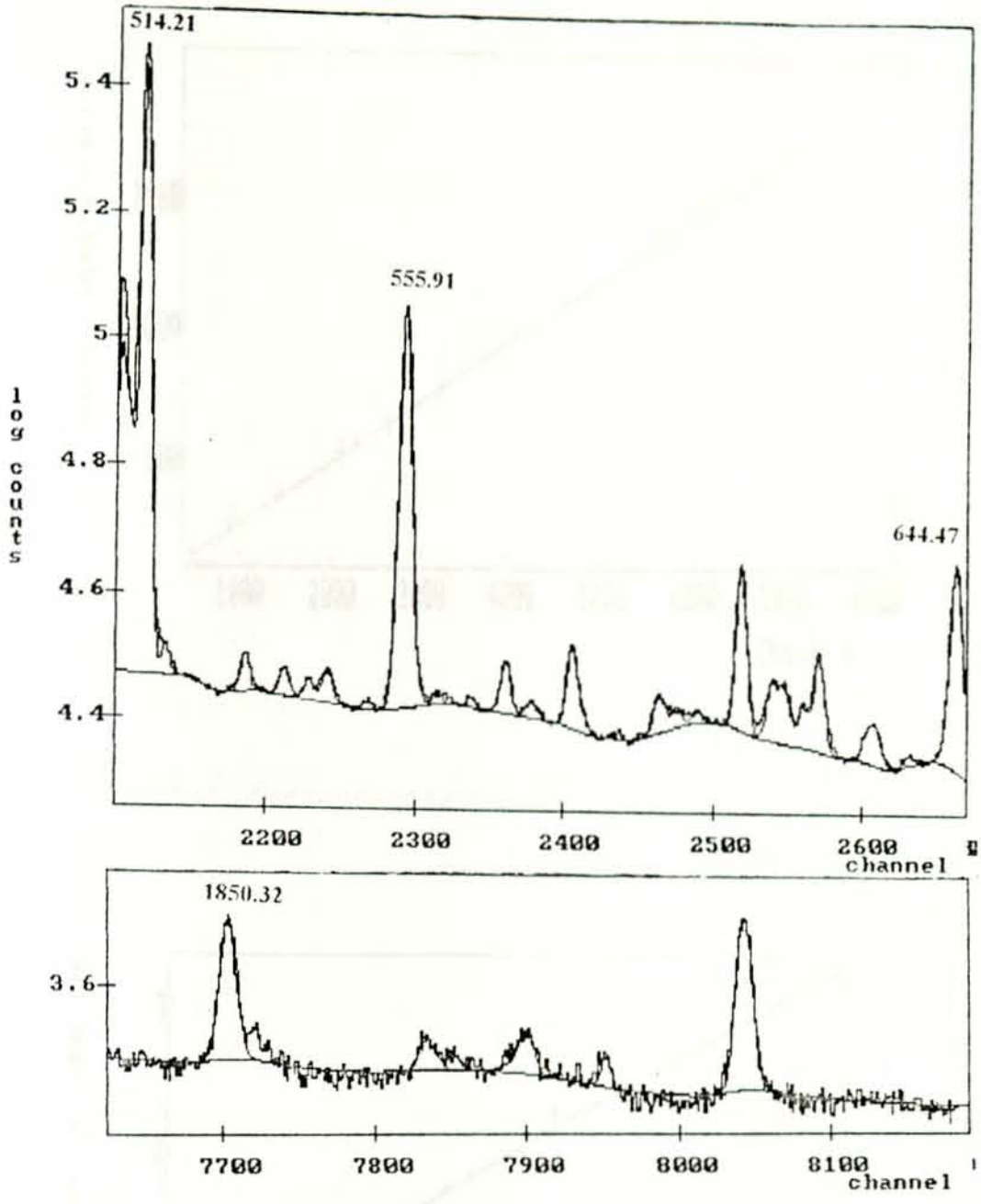

Fig 15 Portion of lines selected from the 90° spectra for energy calibration. Their respective energy in keV is indicated.

By selecting a total of thirteen lines of this type the energy calibration was made. The resulting energy calibration curve generated to analyse the 90° spectrum is depicted in fig. 16

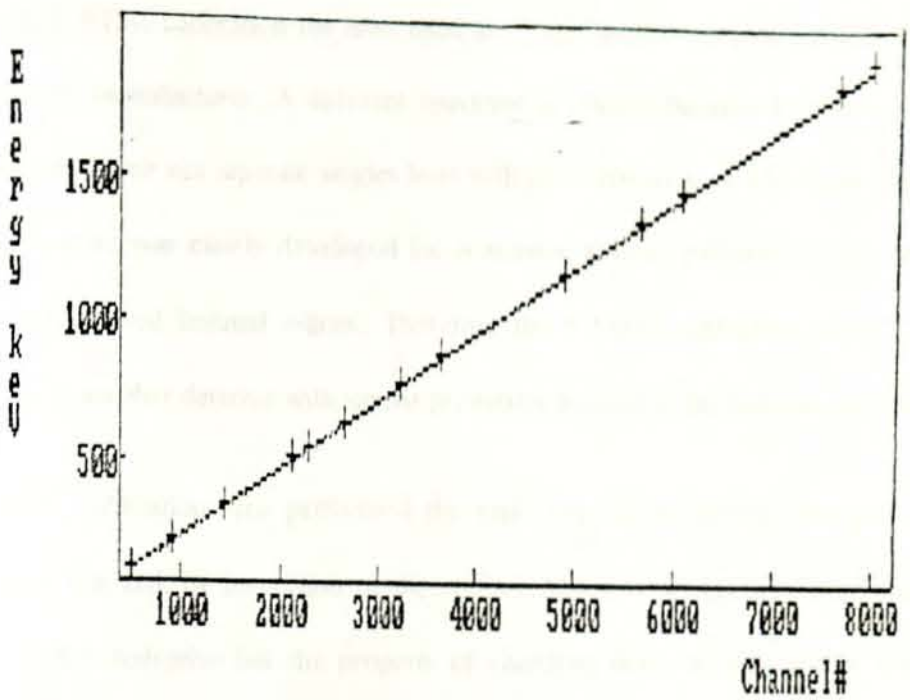

Fig. 16 Energy calibration curve for the Co spectrum

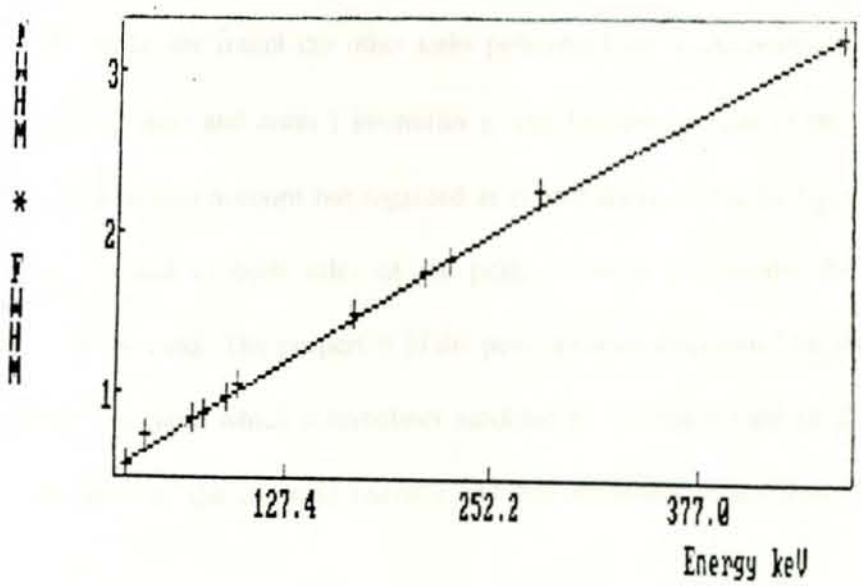

Fig. 17 FWHM calibration curve.

For the FWHM calibration the lines used are from another spectrum which is prepared by GANAAS manufacturer. A different spectrum is chosen because the lines of the in-beam measurement are not separate singles lines with good statistics, as it is required in GANAAS. This software was mainly developed for activation analysis purposes, where one deals with only a few, well isolated γ-lines. Therefore the FWHM calibration curve (see fig.17) belongs to another detector with similar properties as used in the in-beam experiment.

After the calibrations are performed the task done is to identify the peaks. GANAAS performs this task by inspection of the second derivative of the measured γ-ray spectrum. The second derivative has the property of changing twice its sign within a peak and the computer is asked to search for such patterns. In order to apply this method to a spectrum with statistical uncertainties the second derivative is smoothed by the appropriate methods [1].

Once the peaks are found the other tasks performed are to determine their exact positions (centroid energies) and areas (intensities). The low-energy tails of the γ-ray lines are not explicitly taken into account but regarded as contributions to the background. A polynomial function is fitted to both sides of the peak in order to describe the total background underneath the peak. The properties of the peak are then determined by fitting the lines using a Gaussian function, which is sometines modified to account for the small asymmetry of the peak. In this way the centroid energies and the intensities of the peaks in the spectra are determined.

3. Results and Discussion

The influence of the Doppler effect found on the shape of many lines of the spectra is indicated in Fig.18a and 18b in the energy interval between 600 and 800 keV.

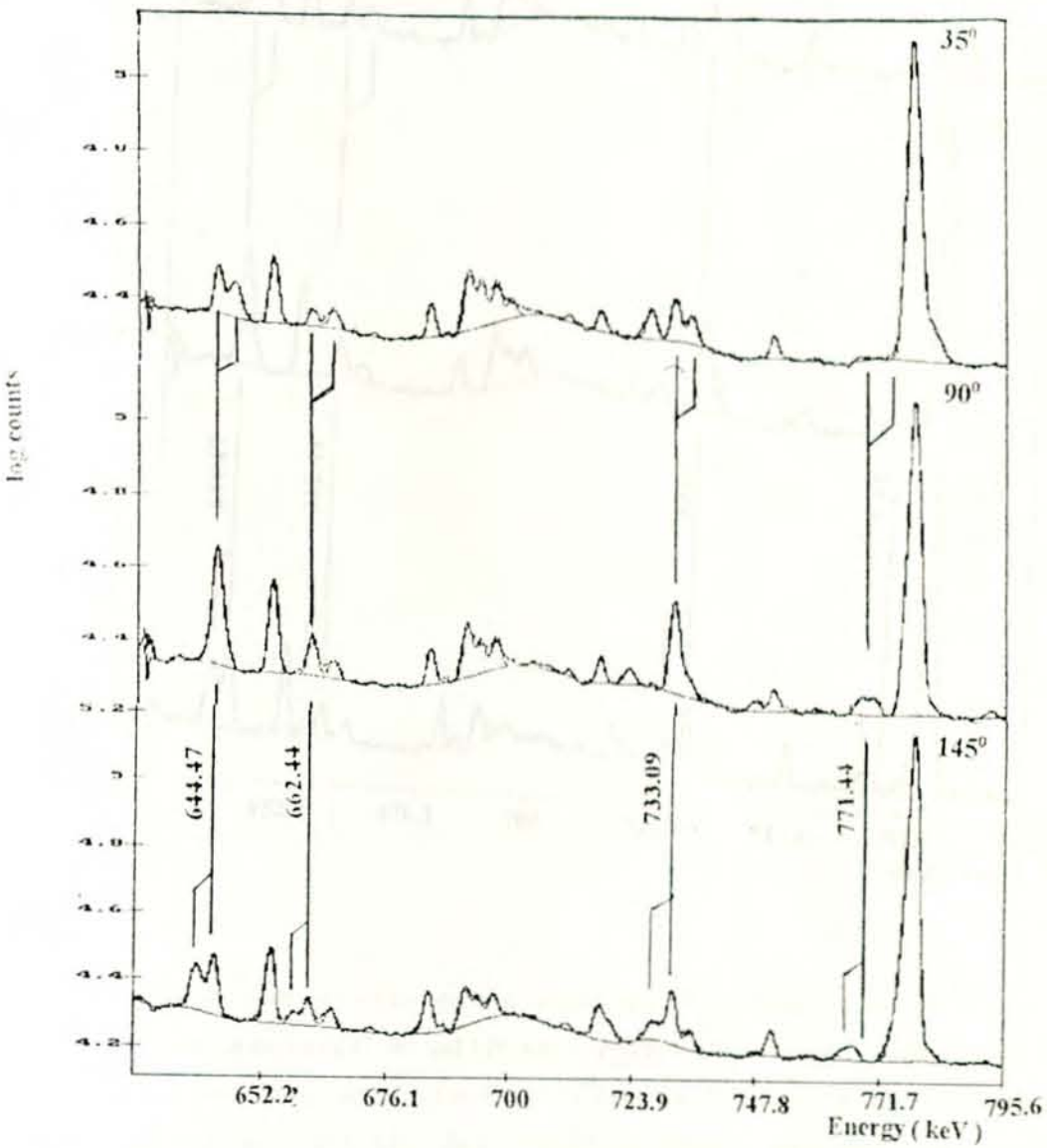

Fig. 18a Portions of singles γ-ray spectra measured during the irradiation of [illegible] with 38 MeV protons at angles of 35°, 90° and 145° with respect to the beam direction. Vertical lines are drawn to point to the influence of the Doppler effect on the lineshape. In the figure is shown an example, where the Doppler effect is difficult to see (at energy 771.44 keV), because in case of the 35° spectrum the shift moves into the direction of a large-intensity line. Clear effects are also seen for the other labled lines.

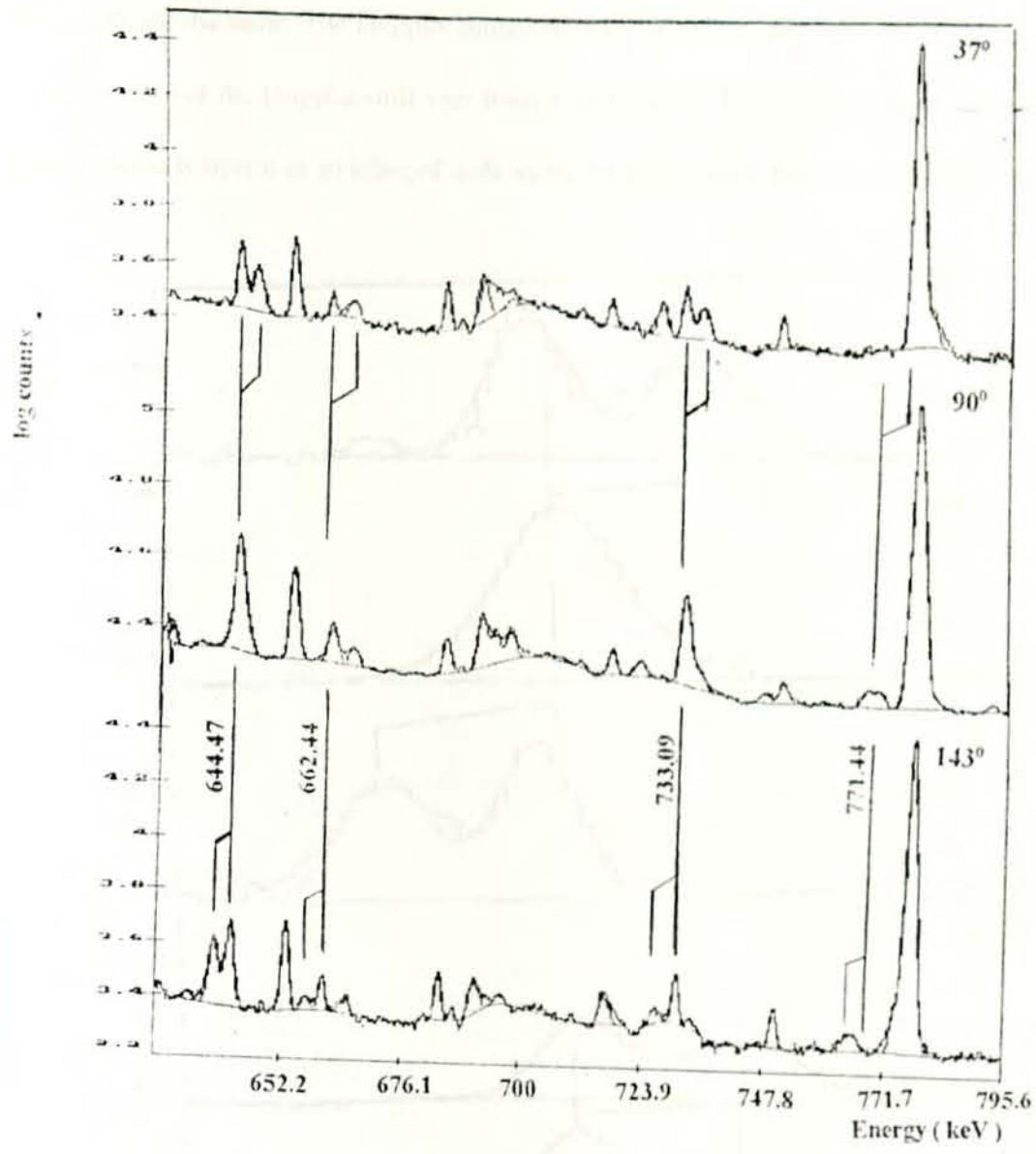

Fig. 18b Portions of singles γ-ray spectra measured during the irradiation of ^{nat}Se with 38 MeV ^{7}Li ions at angles of 37°, 90° and 143° with respect to the beam direction. Vertical lines are drawn to point to the influence of the Doppler effect on the lineshape of the peaks. In the figure is shown an example, where the Doppler-effect is difficult to see (at energy 771.44 keV), because in case of the 37° spectrum the shift moves into the direction of a large-intensity line.

The linehape analysis of the spectra at 37° , 90° and 143° and the resulting shifted lines depicted in fig.18b shows the same result as published in [10]: that is lines at which the

shifts occur are the same. The Doppler shifted lines for all spectra are listed in Tables 3 (a d). The values of the Doppler shift vary from 1 to 4.5 keV. The Doppler effect changes of the lines shape is shown in an inlarged scale including only a small number of peaks (see fig. 19).

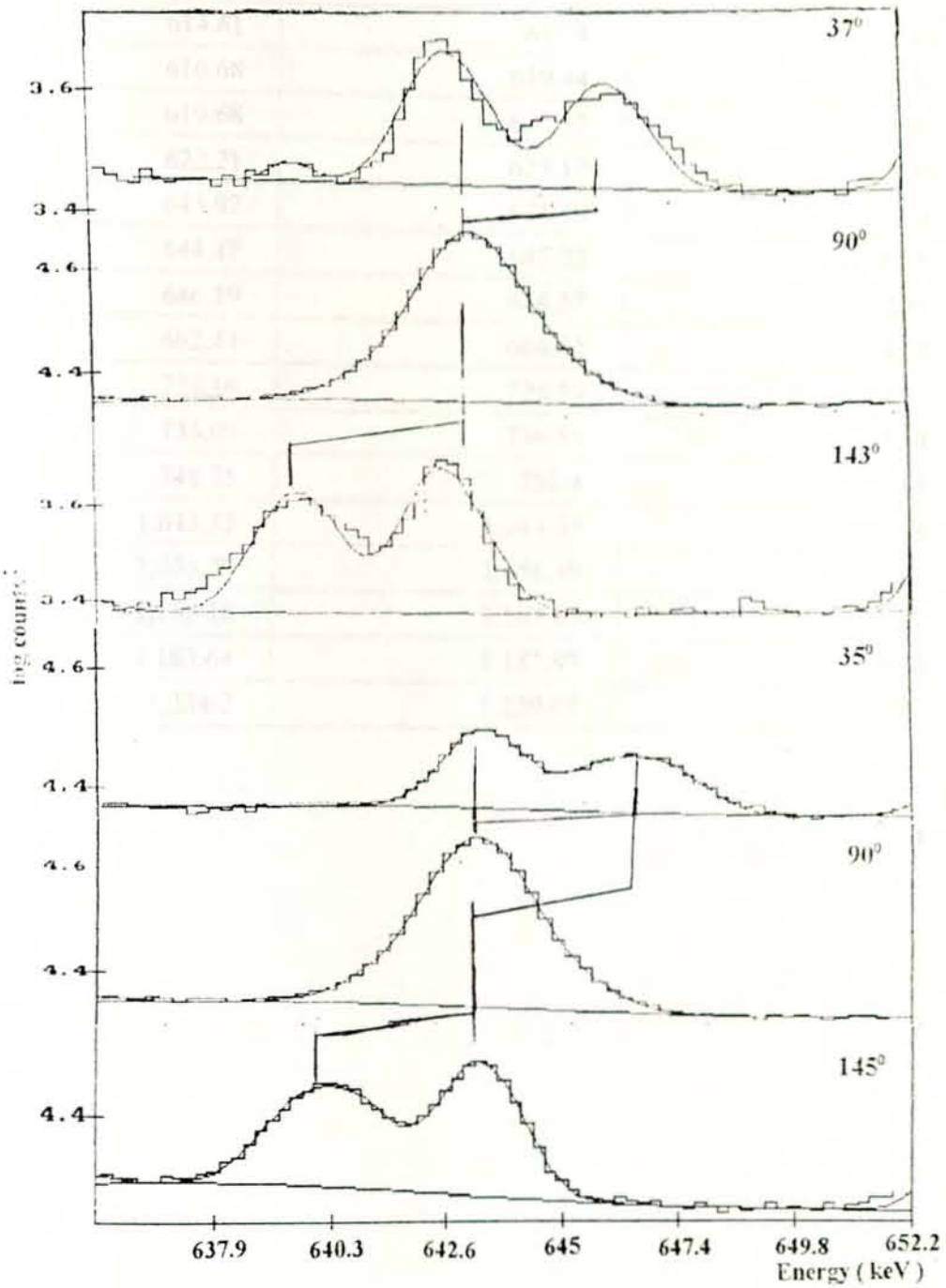

Fig. 20 Doppler-shift of the line of 11.47 keV

Table 3a Doppler shifted lines found in the 35° spectrum

$E_{\gamma 0}$ [keV]	E_γ (35°) [keV]	ΔE_γ [keV]
151.24	153.12	1.88
356.84	358.96	2.12
514.21	516.92	2.71
614.61	617.1	2.49
616.68	619.44	2.76
619.68	622.57	2.89
622.21	625.17	2.96
643.02	644.70	1.68
644.47	647.22	2.75
646.19	648.57	2.38
662.44	666.62	4.18
724.16	728.59	4.43
733.09	736.53	3.44
748.75	752.4	3.65
1,043.35	1,044.35	1
1,055.29	1,058.49	3.2
1,162.16	1,163.65	1.49
1,183.64	1,187.97	4.33
1,234.2	1,239.07	4.87

Table 3b Doppler shifted lines found in the 37^0 spectrum

$E_{\gamma 0}$ [keV]	$E_\gamma(37^0)$ [keV]	ΔE_γ [keV]
149.98	151.33	1.26
514.21	515.55	1.24
614.61	616.58	1.85
616.68	618.58	1.69
619.68	621.73	2.05
622.21	624.95	2.63
644.47	647.25	2.79
662.44	666.02	3.58
724.16	727.68	3.35
733.09	735.72	2.63
1,183.64	1,185.04	1.4
1,288.3	1,290.04	1.75

Table 3c Doppler shifted lines found in the 143° spectrum.

$E_{\gamma 0}$ [keV]	E_{γ} (143°) [keV]	ΔE_{γ} [keV] -
149.98	147.04	2.79
151.24	147.04	4.05
193.9	192.77	1.13
631.62	630.04	1.58
643.02	640.76	2.26
644.47	643.37	1
777.47	775.38	2.15
782.57	781.2	1.37
1,014.62	1,013.34	1.28
1,031.31	1,029.85	1.46
1,043.35	1,041.92	1.43
1,064.69	1,063.28	1.41
1,071.44	1,069.93	1.51
1,078	1,076.61	1.39
1,096.17	1,094.7	1.47
1,099.88	1,098.31	1.58
1,115.95	1,114.49	1.57
1,174.04	1,172.08	1.96
1,177.11	1,175.59	1.52
1,183.64	1,182.08	1.56
1,214.05	1,212.33	1.72
1,218.28	1,216.92	1.36
1,234.2	1,232.55	1.65
1,261.06	1,259.01	2.05
1,274.36	1,273.03	1.33
1284.36	1,282.53	1.83

Table 3d Doppler shifted lines found in the 145° spectrum

$E_{\gamma 0}$ [keV]	$E_\gamma(145^0)$ [keV]	ΔE_γ [keV]
175.69	172.42	3.27
217.15	215.78	1.37
619.68	617.45	2.23
631.62	630.57	1.05
643.02	640.63	2.39
644.47	641.89	2.58
662.44	659.66	2.78
708.23	706.43	1.8
733.09	729.51	3.58
768.97	766.12	2.85
771.44	768.18	3.26
777.53	775.78	1.75
1,014.62	1,011.47	3.15
1,017.53	1,014.58	2.57
1,081.9	1,078.1	3.8
1,084.63	1,082.15	2.48
1,261.06	1,257.01	4.05

From the many detected lines those lines whose Doppler shift is identified are listed in Tables 3 (a – d). As indicated in the tables only a small portion of the total of some 300 lines exhibit a Doppler shift by a value from 1 to 4.5 keV. The reason for why the majority of the lines do not exhibit shift may be the longer lifetime of the states. Because, if the lifetime of the state is large nuclei could de-excite only after they are at rest or about to rest. The fact that some of the nuclei may not attain the required recoil speed in order that the shift appears dominantly can also attribute to the absence of the shift. Also, the shift of closely spaced lines

could be hidden from being identified and in so doing contribute to the decrease of the total number of shifted lines.

Considering a shift less than 1 keV may not guarantee that it is from a Doppler shift since this order of magnitude is of the same order of magnitude as the resolution of Ge-detectors. The other reason is that the fitting procedure cannot give a certainty of more than this order. The fitting procedure by itself can give a shift of one or two channel from expected value which is almost of the order of 1 keV.

The shift of the lines ranging from 1 to 4.5 keV is in accordance with eq. 4 If we take the speed of the recoil nuclei to be about 0.005c [1], the corresponding shift amounts definitely to this order.

The identification of the reaction product nuclei is done by comparing the analysed energy values at 90° with that of the nuclear decay scheme of mass region $A \sim 80$ [5, 12, 19]. Most of the reaction product nuclei whose γ-lines have shown a Doppler shift are given in table 4. Their level energies, spin states and lifetime of excited states are also included to give more information about the shifted lines. Calculated values of the Weisskopf estimate of the various shifted transitions, are given in the table. The calculation is only made for the transitions whose lifetime measurement is published in the above mentioned publications.

Table 4 Nuclei whose γ-transition experience Doppler shift together with their level energy, the corresponding gamma transition energy, initial and final spin states, experimental and theoretical lifetime values and order of multipolarity. T_w is calculated using Weisskopf estimate.

Nuclei	E_{lev} (MeV)	E_γ (MeV)	I_i - I_f	T_{ex} (ps)	T_w (ps)	σλ
^{82}Sr	4.142	616.68	8^+ - 7^-	-------	-----	----
	3.525	708.23	7^- - 5^-	-------	-----	----
	5.569	1,218.28	12^+ - 10^+	-----	-----	E2
^{83}Zr	-------	356.84	-----	------	-----	----
	2.360	768.97	-----	-----	-----	----
	2,914	1,096.17	$21/2^+$ - $17/2^+$	-----	-----	E2
	5.644	1,214.05	$29/2^+$ - $25/2^-$	-----	-----	E2
	6.074	1,234.2	$31/2^-$ - $27/2^-$	-----	-------	E2
^{83}Br	-------	1,177.11	-----	-----	------	----
	-------	1,284.36	-----	-----	-----	----
^{83}Y	-----	1,078	-----	-----	-----	----
^{85}Rb	151.2	151.24	$3/2^-$ - $5/2^-$	-----	-----	----
	514	514.21	$9/2^-$ - $5/2^-$	-----	-----	----
	4.757	622.21	$25/2$ - $23/2$	0.3	0.13	M1
	4,135	644.47	$23/2^+$ - $21/2^-$	0.1	0.11	M1
	3,717	662.44	-----	-----	-----	----
	6,335	724.16	$31/2^+$ - $29/2^+$	0.2	0.08	M1
	7,106	771.44	$33/2^-$ - $31/2^+$	0.06	0.07	M1
	3,491	1,014.62	$21/2^+$ - $17/2^+$	8	0.34	E1
	2.476	1,183.64	$17/2^-$ - $13/2^-$	1.1	16	E2
^{85}Kr		1,261.06	-----	-----	-----	---
^{86}Rb	2,416	733.09	9^+ - 8^-	0.35	0.08	M1
	1,558	777.47	7^+ - 7^-	-----	-----	----
	35.78	1,162.16	10^+ - 9^-	-----	------	M1
^{86}Sr	-------	619.68	4^- - 5^-	-----	-----	---
^{86}Kr	4,430	614.61	6^- - 5^+	-----	-----	----
^{88}Mo	7,322	1,115.95	16^+ - 14^+	-----	-----	----

For some of the lines which are found to show Doppler shift the value of their energies at different angles are shown in figs. 20(a -f). Their fitting parameters are given together with the graphs.

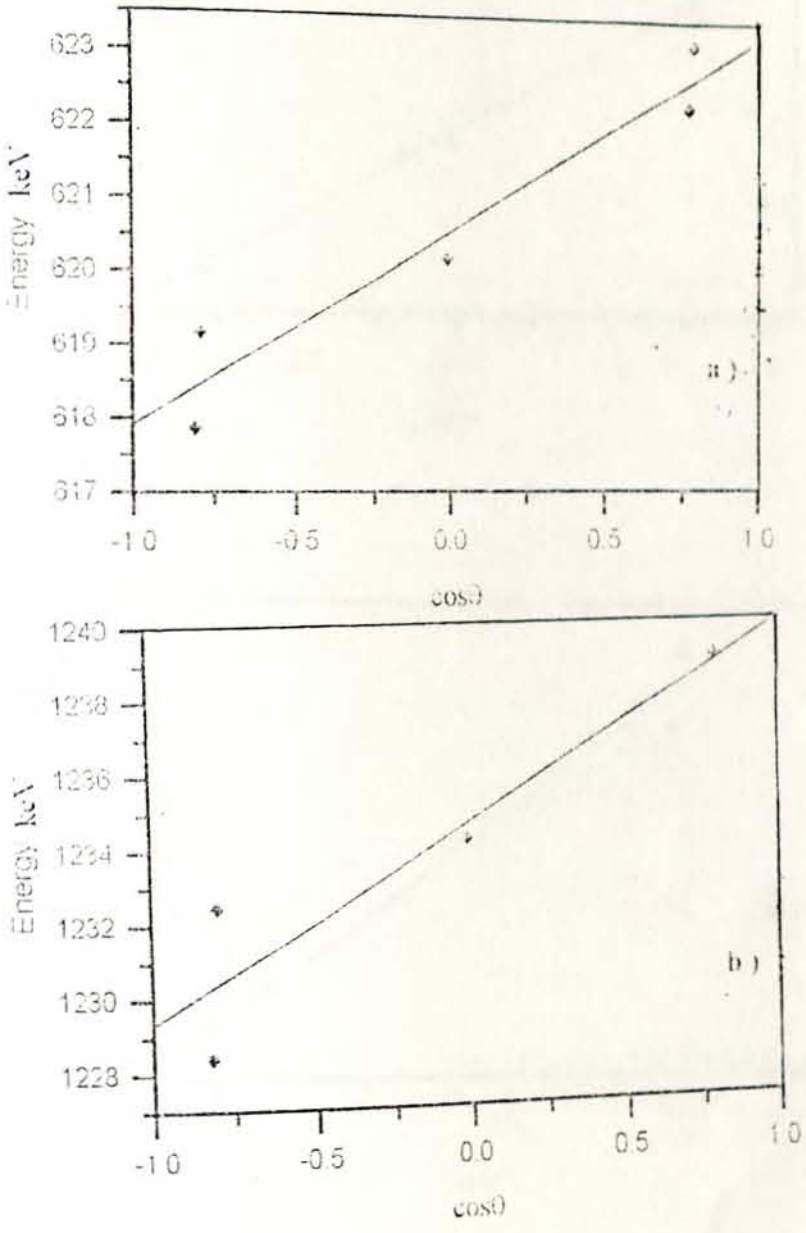

Fig. 20 E_γ vs cosθ plot for : a) 619.83 keV γ-rays from ^{97}Sr nuclei b) 1231.21 keV γ-rays from ^{97}Zr nuclei. The coefficients of determination for the fitting are 0.96 and 1.0 respectively.

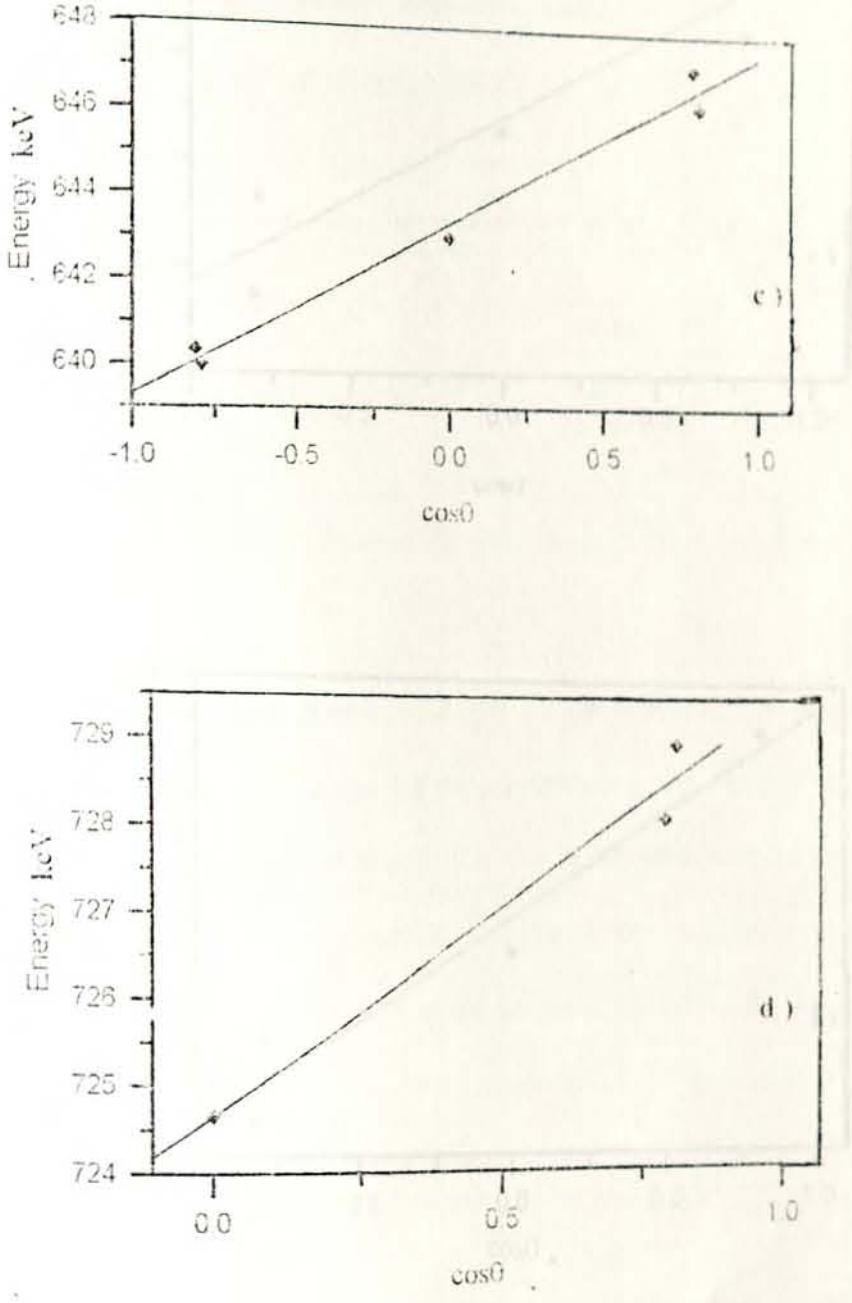

Fig. 20 E_γ versus cosθ plot for: c) 643.98 keV γ-lines d) 724.16 keV γ-lines from ^{82}Rb

The coefficient of determination for the fitting are 0.99 and 1.0 respectively.

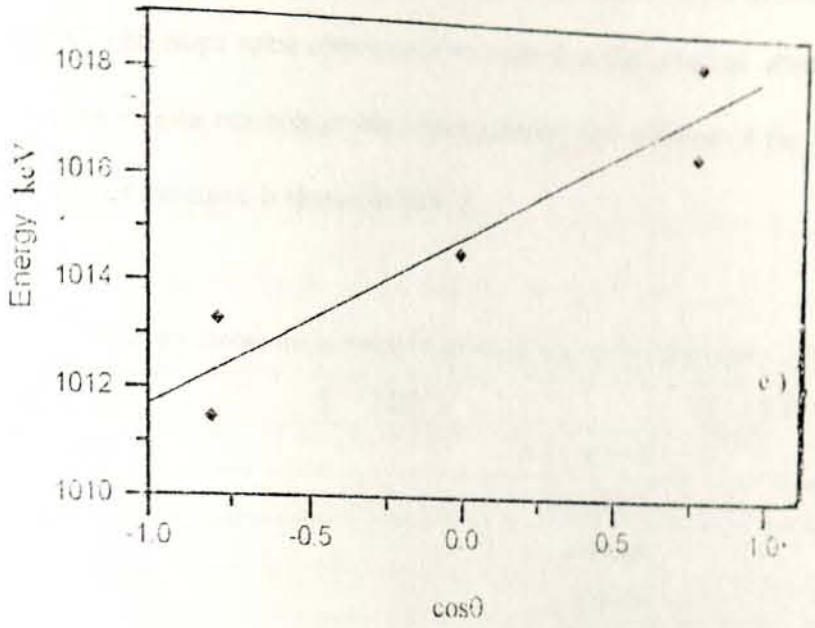

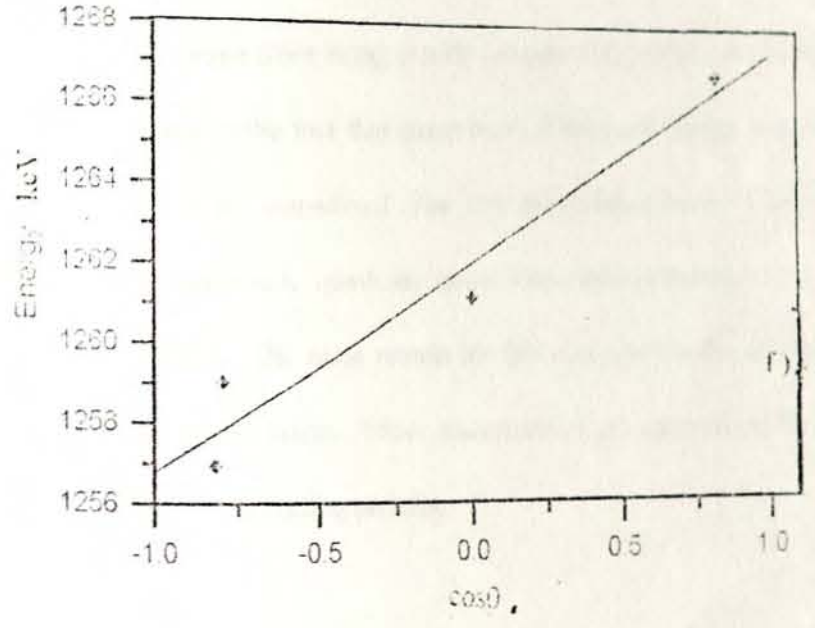

Fig. 20 E_γ versus cosθ plot for: e) 1014.62 keV γ-lines from ^{87}Rb f) 1261.97 keV γ-lines from ^{85}Kr nuclei. The coefficient of determination for the fitting are 0.91 and 0.97, respectively.

The graphs are linear with good quality of fitting. Their slope being in the order of magnitude of 10^{-3} MeV. This slope value corresponds to a recoil nuclei speed of about 0.01c. The v / c values of the various reaction product nuclei during the emission of the γ-lines calculated from the slope of the curve is shown in table 5.

Table 5 (v / c) values for various nuclei during the emission of certain Doppler shifted lines

Nuclei	E_γ (MeV)	v / c (x 10^{-3})
^{85}Rb	1,183.64	2.3
^{83}Zr	1,234.2	4.2
^{86}Sr	619.68	4.1
^{85}Kr	1,261.06	4
^{82}Sr	616.68	4.9
^{86}Rb	733.09	5.5

The deviation of the graph from being exactly straight with coefficient of determination value different from 1 is due to the fact that linear relation between energy and channel number in calibration procedures are considered. The real dependence between channel number and energy has a small magnitude quadratic term. This term contributes to a correction from 0.055 keV to 0.115 keV. The main reason for this correction is the deviation from linearity of the amplifier analyzer system. These uncertainties are ignored in the analysis, as it is usually done, to simplify the fitting process.

The fact that E_γ versus $\cos\theta$ plot is a straight line, to a good approximation is an important feature of Doppler shift because the slope of the curve makes the calculation of Doppler shift attenuation factor $F(\tau)$ in solids possible, an important parameter in DSAM measurements.

Conclusion

The emitted γ-rays from different reactions of ^{82}Se (^{7}Li, xn) produce a characteristic lineshape in the detector which depends on its angle of emission relative to the incident beam, and on the initial recoil speed. Lineshape analysis of the observed spectra using visual inspection enable the identification of the Doppler shifted lines. Many lines have shown this effect with a shift ranging from 1 keV up to 4.5 keV. Eventhough there is no well defined and straight forward technique for identifying Doppler shifted lines a combined effort of personal judgment and the use of a computer provided the possibility to find out the shifted lines. Since individual line judgment can be subjected to errors, the results obtained in this work cannot be free from this drawback. However, in general terms, from comparison with many of the results which are found in literature, it is certain that correct analysis procedures and results have been obtained.

REFERENCES

[1] W. Greiner and M. Eisenberg, " Nuclear Models ", Vol.I, North Holland Publishing Company, Amsterdam (1970).

[2] D. Pelte and D. Schwalm, " In Beam Gamma-ray Spectroscopy with Heavy Ions ", in Heavy Ion Collisions: Vol. III, North-Holland Publishing Company, Amsterdam (1982).

[3] M. Blatt and V. Weisskopf, " Theoretical Nuclear Physics ", John Wiley and Sons, Inc. (1966).

[4] M.A Preston, " Physics of the Nucleus ", Addison-Wesley Publishing Company, Inc., London (1962).

[5] D.H. Wilkinson, " Nuclear Spectroscopy ", Part B, " Academic Press, Inc., London (1970).

[6] F. Ajzenberg-Selove " Nuclear Spectroscopy ", Academic Press, New York and London (1960).

[7] J.Keinonen, K.P Lieb and H.P.Hellmeister, Nucl. Phys. A 376 (1982) 246.

[8] A. Jungclaus, T. Belgya, D.P. Diprete, M.Villani, E.L. Johnson, E.M. Baum, C.A. McGrath, S.W. Yates and N.V. Zamfir, Phys.Rev. 48 C (1993) 1005.

[9] T. Fenyes, " Nuclear Structure, Reactions, and Symmetries", Vol 2 , World Scientific, Dubrovnik (1986).

[10] G.Winter, J.Döring, F. Dönau and L. Funke, Z. Phys. A-Atomic Nuclei 334, (1989) 415.

[11] K.W Allen, " Measurement of Short Nuclear Lifetimes with Lithium-Drifted Germanium Detectors", International Atomic Energy Agency, Vienna (1966).

[12] S. L. Tabor, J. Döring, J. W. Holcomb, G. D. Johnson et.al. Phys. Rev., C49 (1994) 730.

[13] G. Winter, R. Schwengner, J. Reif and H. Prade, Phys. Rev. C49 (1994) 2427.

[14] S. L Tabor, J. Döring, J. W. Holcomb, G. D. Johnson, et.al. Phys. Rev. C49 (1994) 730.

[15] C. A. Fields and F. W. N. De Boer, Nucl. Phys. A 398 (1983) 512.

[16] K. O. Zell, J. W . Peters, W. Gast, H. W. Schuch, and P. Von Brentano, Phys. Rev. C 25 (1980) 1379.

[17] M. Weiszflog, K. P. Lieb, F. Cristancho, C. J. Gross, A. Jungclaus, et.al., Z. Phys. A Hadrons and nuclei 342, (1992) 257.

[18] C. J. Lister, B. J. Varley, W. Fiber, J. Heese et.al., Z. Phys. A- Atomic Nuclei 329, (1988) 413.

[19] D. Rudolph, C. J. Gross, K. P. Lieb, W. Gelletly, M. A. Bently, Z. Phys. A-Hadrons and Nuclei 338, (1989) 139.

Appendix A

1. Gamma Activity and Neutron Activation Analysis System (GANAAS) consists of many modules (see fig. 21). From all these the relevant ones in the analysis of the data are Parameters Setup and Analysis Routines.

Parameters setup routines include different calibration procedures, and result in an input file which specifies all the parameters required for analysis of a spectrum. The analysis program on the other hand permits the selection of the appropriate input file, and the spectra to be analysed, performs the gamma ray spectrum analysis, and displays the results. The results of analysis are stored in a file so that it could be refereed to at any time.

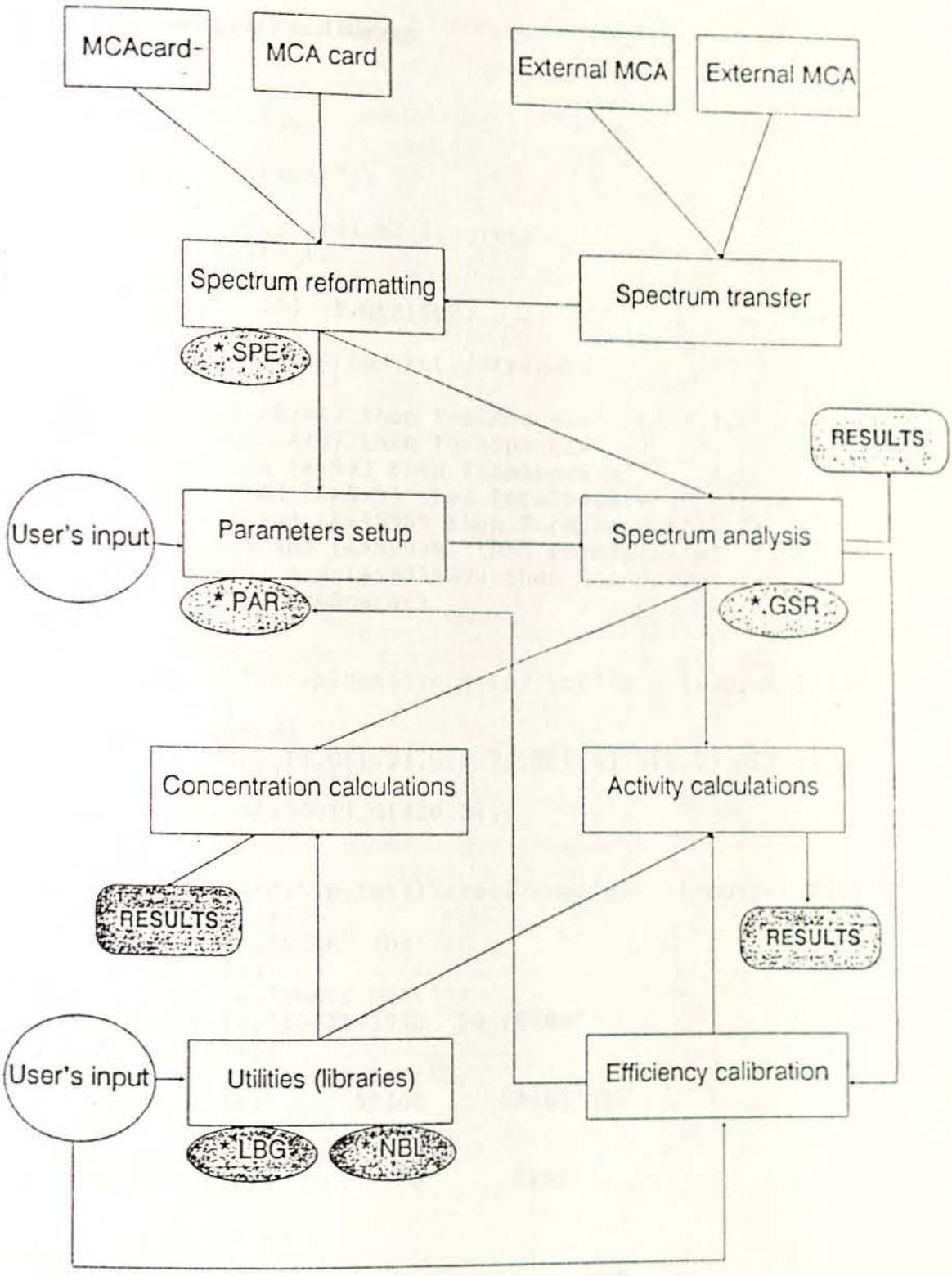

Fig. 21 Structure and organization of GANAAS

2. A programme used to transfer the spectra into a form readable by GANAAS. The programme is written in Pascal language.

```
program correction;
uses crt;
type string7=string[7];
var
G: array[1..820,1..10] of longint;
infile,outfile:text;
i,k:integer;
Space:array[1..10] of string7;

function FormSpace(A:longint):string7;
begin
  if(A<10) and (A>-1) then FormSpace:='       ';
  if(A<100) and (A>9) then FormSpace:='      ';
  if(A<1000) and (A>99) then FormSpace:='     ';
  if(A<10000) and (A>999) then FormSpace:='    ';
  if(A<100000) and (A>9999) then FormSpace:='   ';
  if(A<1000000) and (A>99999) then FormSpace:='  ';
  if(A<10000000) and (A>999999) then FormSpace:=' ';
end; {-function FormSpace-}

begin {-Main-}
assign(infile,'C:\tp\kotel\spect37.txt');   {-input file-}
reset(infile);
for i:=1 to 819 do
read(infile, G[i,1],G[i,2],G[i,3],G[i,4],G[i,5],G[i,6],G[i,7],
G[i,8],G[i,9],G[i,10]);
readLn(infile,G[820,1],G[820,2]);
close(infile);

assign(outfile,'C:\tp\kotel\spec37.spe');   {-output file-}
rewrite(outfile);
writeLn(outfile,'$SPEC ID:');
writeLn(outfile);
writeLn(outfile,'$DATE MEA:');
writeLn(outfile,'10-31-1990  10:16:00');
writeLn(outfile);
writeLn(outfile,'$MEAS TIM:');
writeLn(outfile,'     50400     50469');
writeLn(outfile);
writeLn(outfile,'$DATA:');
writeLn(outfile,'          0      8191');

for i:=1 to 819 do
begin
  for k:=1 to 10 do Space[k]:=FormSpace(G[i,k]);
  for k:=1 to 9 do write(outfile,Space[k],G[i,k]);
  writeln(outfile,Space[10],G[i,10]);
end;
for k:=1 to 2 do Space[k]:=FormSpace(G[820,k]);
writeLn(outfile,Space[1],G[820,1],Space[2],G[820,2]);

close(outfile);
end.
```

Appendix B

Table 6 Lines selected from the spectra at 35 to setup parameters using the energy calibration. Lines whose nuclei identified are indicated.

#	Channel #	Entered Energy (keV)	Fitted energy (keV)	Nuclei
1	494.85	125.62	125.49	------
2	795.45	197.4	197.48	------
3	909.58	224.67	224.81	------
4	1,433.53	350.04	350.26	^{85}Rb
5	2,115.13	514.17	513.44	^{85}Rb
6	2,292.7	555.56	555.95	^{88}Y
7	3,226.47	779.51	779.45	^{85}Rb
8	3,655.81	882.14	882.2	------
9	4,916.45	1,183.84	1,183.84	^{88}Mo
10	6,089.23	1,464.26	1,464.38	------
11	7,703.58	1,850.42	1,850.44	------
12	8,043.37	1,931.76	1,931.68	------

Table 7 Lines selected from the spectra at 37° to setup parameters using the energy calibration. Lines whose nuclei identified are indicated

#	Channel #	Entered energy (keV)	Fitted energy (keV)	Nuclei
1	495.97	125.62	125.7	------
2	777.05	193.09	192.99	^{85}Rb
3	910.29	225.15	224.89	------
4	1,433.3	349.8	350.1	------
5	2,117.27	513.93	513.83	^{85}Rb
6	3,223.31	778.54	778.55	^{85}Rb
7	3,651.16	880.95	880.93	------
8	4,153.85	1,001.05	1,001.22	------
9	4,909.58	1,181.69	1,182.03	^{88}Mo
10	6,075.51	1,461.62	1,460.92	------
11	7,691.21	1,847.06	1,847.31	------
12	8,030.44	1,928.41	1,928.41	------

Table 8 Lines selected from the spectra at 90° to setup parameters using the energy calibration. Lines whose nuclei identified are indicated.

#	Channel #	Entered energy (keV)	Fitted energy (keV)	Nuclei
1	494.8	125.38	125.43	------
2	909.35	224.67	224.66	------
3	1,432.9	350.04	349.98	^{85}Rb
4	2,118.25	514.17	514.02	^{85}Rb
5	2,292.88	555.8	555.82	^{88}Y
6	2,663.06	644.32	644.41	^{85}Rb
7	3,226.34	779.26	779.22	^{85}Rb
8	3,655.87	881.9	882.01	------
9	4,916.43	1,183.6	1,183.63	^{85}Rb
10	5,680.1	1,366.4	1,366.36	------
11	6,089.15	1,464.25	1,464.21	------
12	7,703.73	1,850.41	1,850.43	------

Table 9 Lines selected from the spectra at 143° to setup parameters using the energy calibration. Lines whose nuclei identified are indicated.

#	Channel #	Entered energy (keV)	Fitted energy (keV)	Nuclei
1	495.66	125.62	125.64	------
2	775.05	192.85	192.54	^{85}Rb
3	910.14	224.91	224.89	------
4	1,432.96	349.79	350.07	^{85}Rb
5	2,117.28	513.69	513.9	^{85}Rb
6	3,223.24	778.78	778.62	^{85}Rb
7	3,650.97	880.95	880.98	------
8	4,154.53	1,001.53	1,001.48	------
9	4,909.35	1,181.93	1,182.08	^{88}Mo
10	6,077.75	1,461.85	1,461.58	------
11	7,691.54	1,847.31	1,847.5	------
12	8,029.68	1,928.41	1,928.34	------

Table 10 Lines selected from the spectra at 145° to setup parameters using the energy calibration. Lines whose nuclei identified are indicated.

#	Channel #	Entered energy (keV)	Fitted energy (keV)	Nuclei
1	494.77	125.62	125.4	------
2	795.38	197.39	197.37	------
3	909.79	224.66	224.77	------
4	1,432.93	350.04	350.01	^{84}Rb
5	2,118.82	513.92	514.19	^{85}Rb
6	3,226.81	779.51	779.37	^{85}Rb
7	3.656.14	881.9	882.11	------
8	4,916.85	1,183.6	1,183.74	^{85}Rb
9	5,337.93	1,284.56	1,284.47	^{85}Rb
10	6,089.96	1,464.72	1,464.35	------
11	7,704.21	1,850.42	1,850.38	------
12	8,043.32	1,931.28	1,931.46	------

Declaration

I the undersigned, declare that the thesis is my original work and all relevant sources used for the thesis are duly acknowledged.

Name: Shewaferaw Solomon

Signature: ----------

Place and date of submission: Addis Ababa University June, 1995.

This thesis has been submitted for examination with my approval as university advisor.

Name: Dr. S. Tesfh

Signature: ----------